UNITED STATES
NUCLEAR REGULATORY COMMISSION
WASHINGTON, D. C. 20555

January 22, 1985

Docket Nos: 50-424
and 50-425

APPLICANT: Georgia Power Company

FACILITY: Vogtle, Units 1 and 2

SUBJECT: SUMMARY OF STRUCTURAL AUDIT HELD DECEMBER 4-6, 1984

The staff met with representatives of the applicant and its architect/engineer, Bechtel, December 4-6, 1984 in Norwalk, California to audit the structural design and calculations for Vogtle, Units 1 and 2. Participants are listed in Enclosure 1.

The meeting agenda is included as Enclosure 2. Each presentation of items A through J summarized the Vogtle design report volume, submitted by letter dated October 31, 1984, related to that item. The presentation was followed by staff questions related to calculations and traceability. The slides used in the presentations which were not already included as part of the design report are included as Enclosure 3. Specifically, these slides include summary information of the Vogtle seismic analysis and graphs comparing response spectra using the deconvolution method (S3 and S4 method) and the impedance method with the actual response spectra used in the Vogtle structural design (the curve marked "issued").

The presentations and calculational review resulted in several action items which are listed in Enclosure 4. The applicant provided responses to Action Items 2 and 3 before completion of the audit. These responses are included as Enclosure 5 and 6, respectively. Attachment 1 to Enclosure 6 provides Bechtel's conversion of the equation given in Enclosure 6 to that which was utilized in the Vogtle structural design.

An additional meeting topic was the applicant's responses to staff questions. The completion of Action Item 1 of Enclosure 4 should provide satisfactory response to questions 220.10, 220.13, 220.14, 220.16 and 220.17. Further staff review is necessary of responses to questions 220.4 and 220.24.

Additional information required by the staff in response to several questions as discussed at the audit is enumerated in Enclosure 7. The staff indicated that it would investigate if additional information is required of the applicant beyond that identified in Enclosure 7 in response to questions 220.26 and 220.27 and inform the applicant subsequent to the audit. The remaining responses require no additional information. Enclosure 8 provides additional detail on

the Mononabe-Okabe formula which the applicant utilized to calculate the lateral soil pressure due to an earthquake. The applicant provided the enclosed paper at the audit.

The applicant indicated that it would respond to the remaining action items by letter prior to February 1, 1985. The applicant further indicated that the necessary revisions to the staff questions would be submitted to the staff by FSAR amendment prior to January 31, 1985.

Melanie A. Miller, Project Manager
Licensing Branch No. 4
Division of Licensing

Enclosures:
As stated

cc: See next page

DESIGNATED ORIGINAL

Certified By Angela Hatton

VOGTLE

Mr. Donald Foster
Vice President and Project General Manager
Georgia Power Company
P.O. Box 299A, Route 2
Waynesboro, GA 30830

cc: Mr. L. T. Gucwa
Chief Nuclear Engineer
Georgia Power Company
P.O. Box 4545
Atlarta, Georgia 30302

Mr. Ruble A. Thomas
Vice President - Licensing
Vogtle Project
Georgia Power Company/
Southern Company Services, Inc.
P.O. Box 2625
Birmingham, Alabama 35202

Mr. R. E. Conway
Senior Vice President - Nuclear
Power
Georgia Power Company
P.O. Box 4545
Atlanta, Georgia 30302

Mr. J. A. Bailey
Project Licensing Manager
Southern Company Services, Inc.
P.O. Box 2625
Birmingham, Alabama 35202

Ernest L. Blake, Jr.
Shaw, Pittman, Potts and Trowbridge
1800 M Street, N.W.
Washington, D. C. 20036

Mr. G. Bockhold, Jr.
Vogtle Plant Manager
Georgia Power Company
Route 2, Box 299-A
Waynesboro, Georgia 30830

Mr. James P. O'Reilly
Nuclear Regulatory Commission
Region II
101 Marietta Street, N.W., Suite 2900
Atlanta, Georgia 30323

Mr. William S. Sanders
Resident Inspector/Nuclear Regulatory
Commission
P.O. Box 572
Waynesboro, Georgia 30830

Deppish Kirkland, III, Counsel
Office of the Consumers' Utility
Council
Suite 225
32 Peachtree Street, N.W.
Atlanta, Georgia 30303

James E. Joiner
Troutman, Sanders, Lockerman,
& Ashmore
Candler Building
127 Peachtree Street, N.E.
Atlanta, Georgia 30303

Douglas C. Teper
Georgians Against Nuclear Energy
1253 Lenox Circle
Atlanta, Georgia 30306

Laurie Fowler
Legal Environmental Assistance
Foundation
1102 Healy Building
Atlanta, Georgia 30303

Tim Johnson
Executive Director
Educational Campaign for
a Prosperous Georgia
175 Trinity Avenue, S.W.
Atlanta, GA 30303

Enclosure 1

PARTICIPANTS

NRC

M. Miller
S. Chan
R. Lipinski

Georgia Power Company

D. Hudson

Southern Company Services

J. Bailey
K. Kopecky

Houston Lighting & Power

R. Attar

Bechtel

M. Malcom*
O. Gurbuz
D. Houghton
D. Jagannathan
N. Joonejo
S. Cereghino*
R. Kosiba*
M. Perovich*
R. Platoni*
L. Hersh*
J. Purucker
R. Schilling*
M. Hutchinson*
A. Palmquist*
M. Patterson*
S. Jeng*
W. Hughes
A. Lim*
S. Patel*
P. Roy*
G. Wozny*
M. Massman*
D. Berd*
M. Lock*
M. Muska*
M. Miller*
D. Falgren*
D. Haavik*

*Attended on a part time basis

Enclosure 2

VOGTLE ELECTRIC GENERATING PLANT - UNITS 1 AND 2
DOCKET NOS. 50-424 AND 50-425

AGENDA

NRC SER AUDIT MEETING
STRUCTURAL AND GEOTECHNICAL ENGINEERING BRANCH

Week of December 3, 1984

			Presenter
Tuesday:	I.	INTRODUCTION	
	II.	REVIEW OF STRUCTURAL DESIGN REPORT AND AUDIT ITEMS	
		A. Brief Overview of Entire Plant	Mike Perovich
		B. Seismic Analysis Report	Jagan
		C. Containment Building	Mike Hutchinson
Wednesday:		D. Containment Internal Structure	Allen Palmquist
		E. Auxiliary Building	Martin Muska
		F. Fuel Building	Martin Muska
		G. Control Building	Suhash Patel
Thursday:		H. Diesel Generator Building	Martin Muska
		I. Category I Tanks	Mark Massman
		J. Other Category I Structures	Mark Massman George Wozny
	III.	REVIEW OF RESPONSES TO NRC QUESTIONS	
	IV.	SUMMARY	M. Perovich Jagan D. Houghton

SEISMIC ANALYSIS REPORT

- INTRODUCTION
- DESIGN BASES
- MATERIAL PROPERTIES
- STRUCTURE MODELS
- SEISMIC INPUT
- SOIL-STRUCTURE INTERACTION ANALYSES
- SEISMIC WAVE PROPAGATION EFFECTS
- EFFECTS OF FLOOR FLEXIBILITY ON RESPONSE SPECTRA
- MISCELLANEOUS ANALYSIS
- CONCLUSION

Enclosure 3

DESIGN BASES

GENERAL

- PSAR SUPPLEMENTS S3 (NOV. 15, 1977) AND S4 (JAN. 25, 1978)
- FEB. 20, 1978 GPC LETTER
  - 1.5 SCALING FACTOR
- MARCH 27, 1978 NRC LETTER
  - ACCEPTANCE FOR PSAR S3 & S4 SUBJECT TO:
    - 1.5 SCALING FACTOR
    - CONFIRMATORY STUDY
    - SENSITIVITY STUDY
    - ADDITIONAL TORSIONAL CONSIDERATIONS
- NOVEMBER 13, 1978 GPC LETTER
  - REPORT ON CONFIRMATORY STUDY
  - REPORT ON "GROUND RESPONSE ANALYSES" COVERING "SENSITIVITY STUDY"
  - METHODOLOGY TO ACCOUNT FOR TORSION CAUSED BY THE SEISMIC WAVE PROPAGATION EFFECTS
- PSAR SUPPLEMENT S5 (NOV. 17, 1978)
  - INCORPORATES 1.5 SCALING FACTOR
- SUMMARY
  - PSAR S3, S4 & S5 & CONSIDERATION OF TORSION DUE TO SEISMIC WAVE PROPAGATION EFFECTS FORM THE BASES FOR SEISMIC DESIGN

DESIGN BASES (CONTD.)

SEISMIC INPUT

- R.G. 1.60 RESPONSE SPECTRA
- PEAK GROUND ACCELERATION OF
  0.2G SSE HORIZONTAL & VERTICAL
  0.12G OBE HORIZONTAL & VERTICAL
- R.G. 1.61 DAMPING VALUES
- R.G. 1.92 – THREE COMPONENT EARTHQUAKE EFFECTS CONSIDERED USING SRSS COMBINATION

SOIL-STRUCTURE INTERACTION EFFECTS

- SHALLOWLY EMBEDDED STRUCTURES
  - IMPEDANCE METHOD
  - CONTROL MOTION APPLIED AT THE FOUNDATION LEVEL IN THE FREE-FIELD
- DEEPLY EMBEDDED STRUCTURES
  - FINITE ELEMENT METHOD FLUSH
  - CONTROL MOTION APPLIED AT THE FINISHED GRADE LEVEL IN THE FREE-FIELD
  - ENVELOPE IN-STRUCTURE RESPONSE SPECTRA TO BE OBTAINED CONSIDERING G, 1.5G AND 1/1.5G
  - ENVELOP SPECTRA MULTIPLIED BY A SCALING FACTOR OF 1.5

SEISMIC WAVE PROPAGATION EFFECTS

- TORSIONAL MOMENTS NO LESS THAN THOSE REQUIRED BY THE UBC ARE TO BE CONSIDERED IN THE DESIGN OF CATEGORY 1 STRUCTURES, EQUIPMENT AND SYSTEMS

SEISMIC WAVE PROPAGATION EFFECTS

CRITERIA

- A STATIC SEISMIC TORSIONAL MOMENT OF NOT LESS THAN THAT REQUIRED BY THE UBC BE CONSIDERED IN ADDITION TO THE EFFECTS RESULTING FROM THE ACTUAL GEOMETRIC ECCENTRICITY

PROCEDURE

- DESCRIBED IN NOVEMBER 13, 1978 GPC LETTER TO NRC
- CATEGORY 1 STRUCTURES
  - IN THE DESIGN OF STRUCTURES, THE ACTUAL ECCENTRICITY AT A GIVEN LEVEL IS INCREASED BY 5% OF THE MAXIMUM PLAN DIMENSION AT THAT LEVEL, AND THE DESIGN STATIC SEISMIC TORSIONAL MOMENT IS COMPUTED AT THE PRODUCT OF THE AUGMENTED ECCENTRICITY AND THE STORY SHEAR
- EQUIPMENT, SYSTEMS AND COMPONENTS
  - THE TORSIONAL MOTION IMPARTED TO THE STRUCTURE AFFECTS ONLY THE HORIZONTAL IN-STRUCTURE RESPONSE SPECTRA USED FOR EQUIPMENT QUALIFICATION
  - EFFECTS CONSIDERED BY ADDING ADDITIONAL
  - HORIZONTAL RESPONSE SPECTRA TO THE HORIZONTAL RESPONSE SPECTRA RESULTING FROM THE THREE COMPONENT EARTHQUAKE EFFECTS, USING ABSOLUTE COMBINATION METHOD

EFFECTS OF FLOOR FLEXIBILITY ON RESPONSE SPECTRA

CONTAINMENT BUILDING

- PURPOSE
  - ASSESS THE EFFECTS, IF ANY, OF THE LOCAL FLEXIBILITY OF THE CONTAINMENT INTERNAL STRUCTURE FLOORS ON THE FLOOR DESIGN RESPONSE SPECTRA

- METHOD
  - 10,000 DYNAMIC DOF 3-D FINITE ELEMENT MODEL OF THE INTERNAL STEEL STRUCTURE COUPLED WITH THE LUMPED PARAMETER MODEL OF THE CONTAINMENT SHELL AND INTERNAL CONCRETE STRUCTURE
  - SOIL-STRUCTURE INTERACTION EFFECTS ARE ACCOUNTED FOR USING THE IMPEDANCE METHOD
  - TIME-HISTORY ANALYSES ARE PERFORMED, AND RESPONSE SPECTRA ARE GENERATED AT THE GOVERNING LOCATIONS ON THE CONTAINMENT FLOORS

- CONCLUSION
  - NO SIGNIFICANT AMPLIFICATION OF HORIZONTAL RESPONSE DUE TO FLOOR FLEXIBILITY
  - THE VERTICAL RESPONSE SPECTRA OBTAINED FROM THIS ANALYSIS ARE ENVELOPED BY THE DESIGN RESPONSE SPECTRA

EFFECTS OF FLOOR FLEXIBILITY ON RESPONSE SPECTRA (CONT'D)

OTHER CATEGORY I STRUCTURES

- PURPOSE
  - EFFECTS OF VERTICAL FLEXIBILITY OF FLOOR SLABS ON THE FLOOR RESPONSE SPECTRA OF SHEAR WALL STRUCTURES
- METHOD
  - TWO DIFFERENT LUMPED MASS STRUCTURE MODELS (ONE RIGID FLOOR MODEL AND ONE FLEXIBLE FLOOR MODEL) ARE USED
  - SOIL-STRUCTURE INTERACTION EFFECTS ARE ACCOUNTED FOR USING THE IMPEDANCE METHOD
  - VERTICAL TIME-HISTORY ANALYSES ARE PERFORMED ON THE TWO MODELS
  - THE STORY RESPONSE SPECTRA FROM THE RIGID FLOOR MODEL ARE COMPARED WITH THE STORY AND FLOOR RESPONSE SPECTRA FROM THE FLEXIBLE FLOOR MODEL
- CONCLUSION
  - EFFECTS OF VERTICAL FLEXIBILITY ON THE FLOOR ACCELERATIONS AND RESPONSE SPECTRA ARE INSIGNIFICANT

MISCELLANEOUS ANALYSES

INTERACTION OF NON-CATEGORY 1 STRUCTURES WITH CATEGORY 1 STRUCTURES

- EQUIPMENT BUILDING
  - DESIGNED TO CATEGORY 1 STRUCTURES CRITERIA
- TURBINE BUILDING, RADWASTE TRANSFER BUILDING
  - DESIGNED FOR SSE CONDITIONS USING CATEGORY 1 STRUCTURES CRITERIA
- CATEGORY 2 TUNNELS
  - DESIGNED TO MAINTAIN THEIR STRUCTURAL INTEGRITY UNDER SSE CONDITIONS

STRUCTURE DISPLACEMENT

- MAXIMUM HORIZONTAL STRUCTURE-TO-STRUCTURE SEISMIC RELATIVE DISPLACEMENT AT ANY ELEVATION IS LESS THAN 2 INCHES
- A STRUCTURE-TO-STRUCTURE SEISMIC GAP OF 5-1/2" SEPARATES ALL CATEGORY 1 BUILDINGS

EVALUATION OF LAYOUT CHANGES

- EVALUATION OF LAYOUT CHANGES IN THE STRUCTURE (AFTER SEISMIC ANALYSIS WAS PERFORMED) IS MADE TO CONFIRM THAT THE CHANGES, IF ANY, IN THE RESPONSE PARAMETERS ARE INSIGNIFICANT

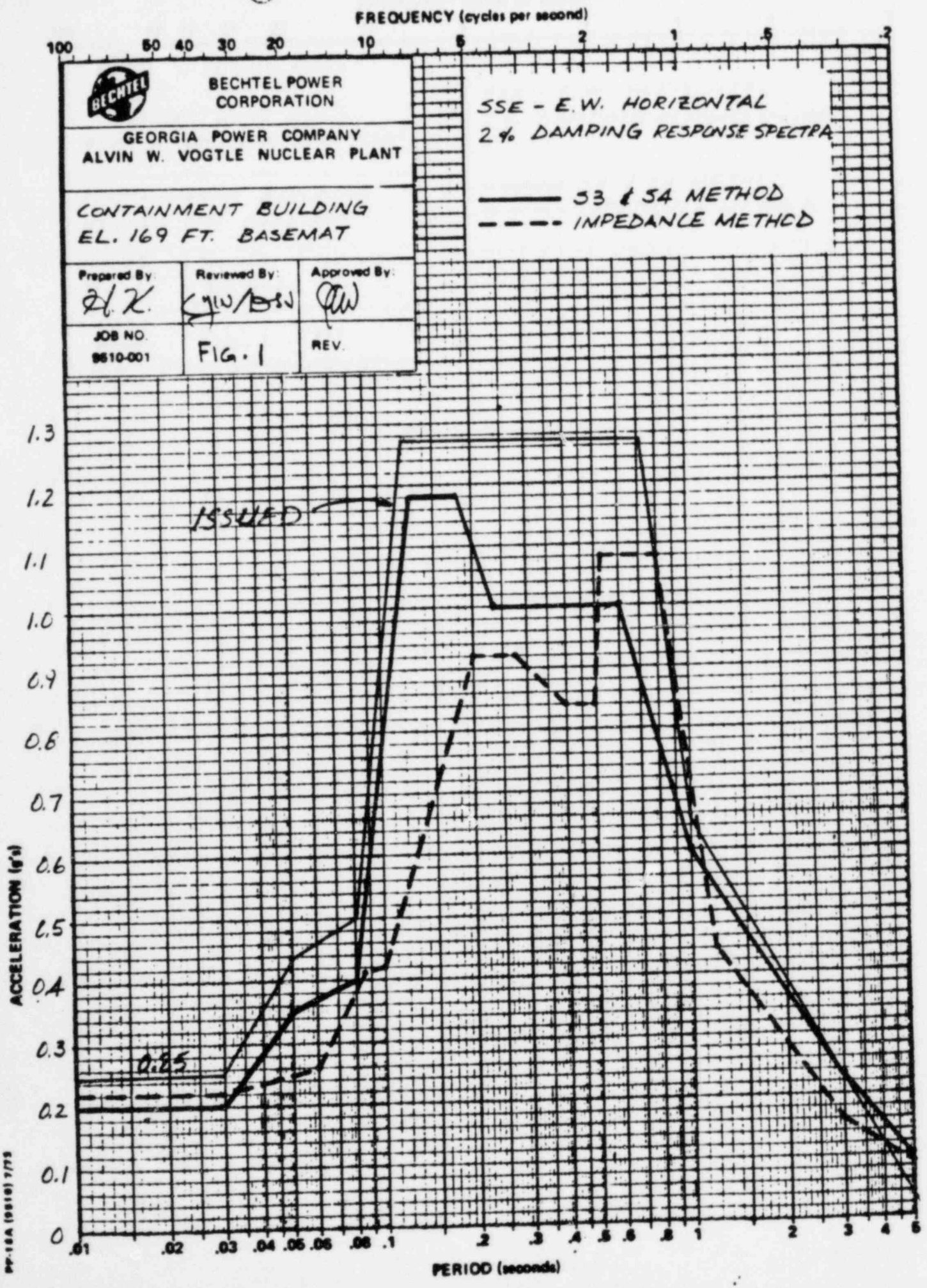
FREQUENCY (cycles per second)
100 50 40 30 20 10 5 2 1 .5 .2
BECHTEL POWER CORPORATION
GEORGIA POWER COMPANY
ALVIN W. VOGTLE NUCLEAR PLANT
CONTAINMENT BUILDING
EL. 169 FT. BASEMAT
Prepared By: A.K.
Reviewed By: CJW/BSN
Approved By: CJW
JOB NO. 9610-001
FIG. 1
REV.
SSE - E.W. HORIZONTAL
2% DAMPING RESPONSE SPECTRA
53 & 54 METHOD
IMPEDANCE METHOD
ISSUED
0.25
ACCELERATION (g's)
1.3 1.2 1.1 1.0 0.9 0.8 0.7 0.6 0.5 0.4 0.3 0.2 0.1 0
.01 .02 .03 .04 .05 .06 .08 .1 .2 .3 .4 .5 .6 .8 1 2 3 4 5
PERIOD (seconds)

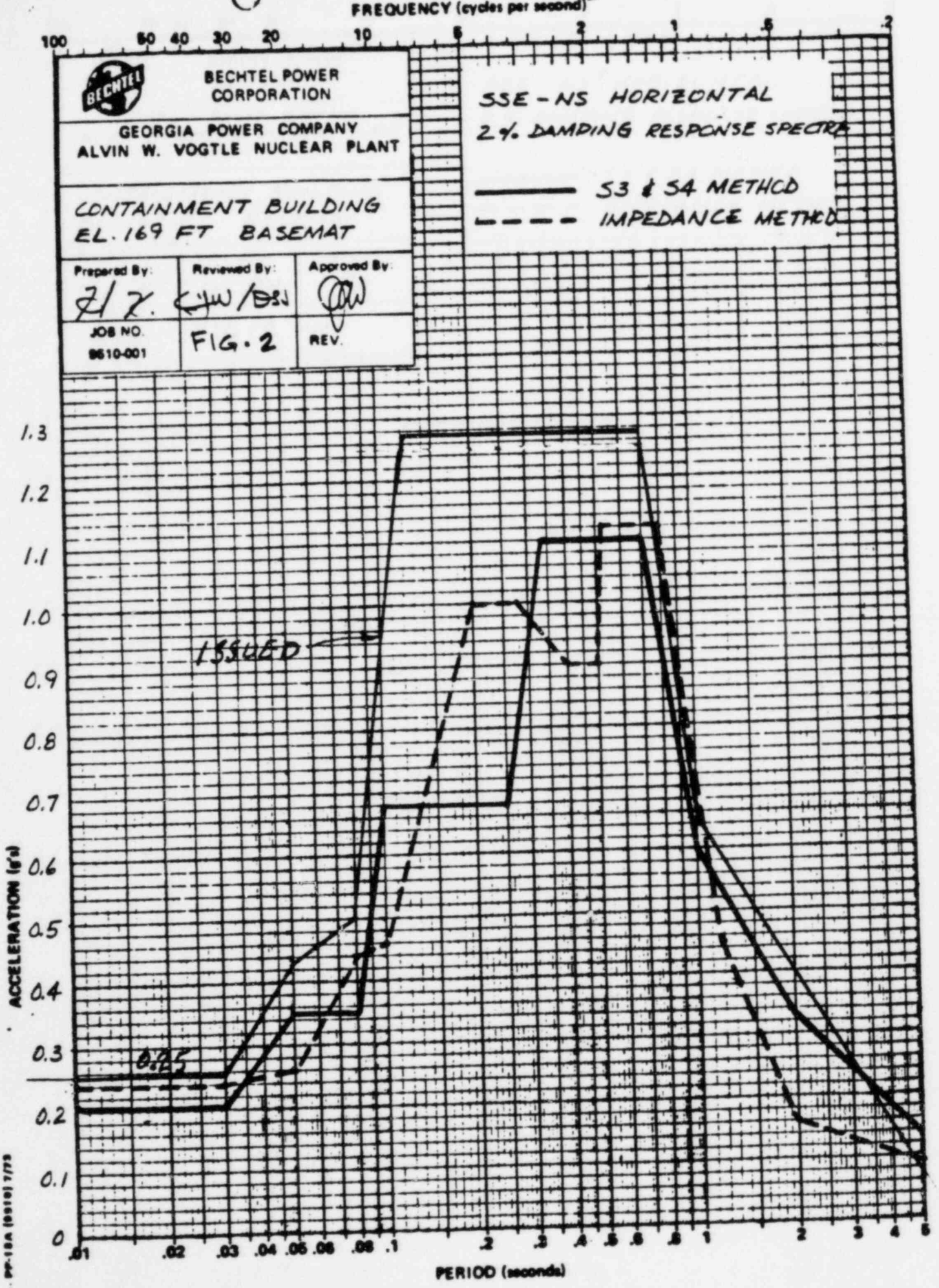
FREQUENCY (cycles per second)
100
50
40
30
20
10
5
2
1
.5
.2
BECHTEL POWER CORPORATION
GEORGIA POWER COMPANY
ALVIN W. VOGTLE NUCLEAR PLANT
CONTAINMENT BUILDING
EL. 169 FT BASEMAT
Prepared By:
Reviewed By:
Approved By:
JOB NO.
9610-001
FIG. 2
REV.
SSE - NS HORIZONTAL
2% DAMPING RESPONSE SPECTRA
S3 & S4 METHOD
IMPEDANCE METHOD
ISSUED
1.3
1.2
1.1
1.0
0.9
0.8
0.7
0.6
0.5
0.4
0.3
0.2
0.1
0
ACCELERATION (g's)
.01
.02
.03
.04
.05
.06
.08
.1
.2
.3
.4
.5
.6
.8
1
2
3
4
5
PERIOD (seconds)

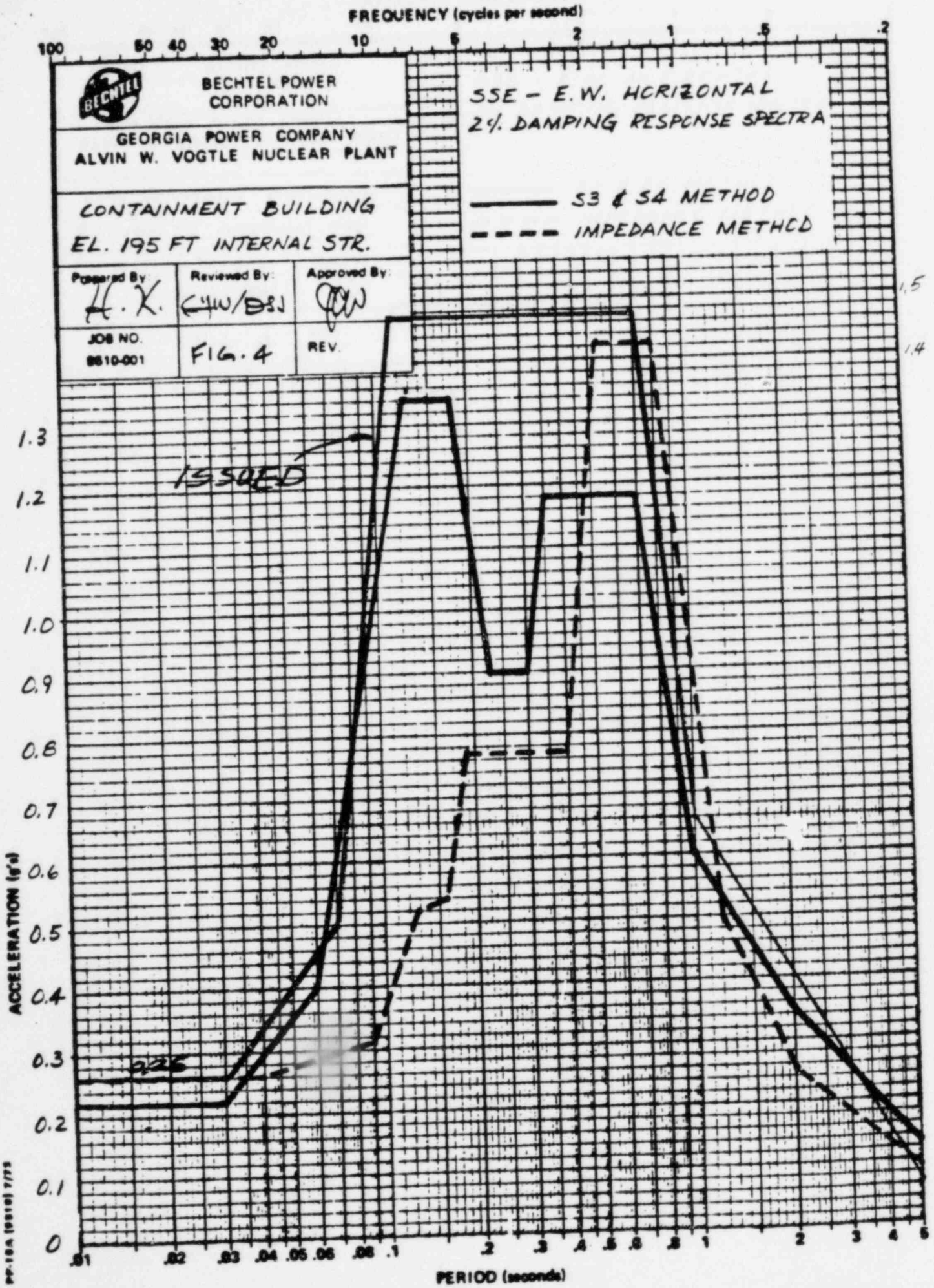
FREQUENCY (cycles per second)
100
50
40
30
20
10
5
2
1
.5
.2
BECHTEL POWER CORPORATION
GEORGIA POWER COMPANY
ALVIN W. VOGTLE NUCLEAR PLANT
CONTAINMENT BUILDING
EL. 195 FT INTERNAL STR.
Prepared By: H. K.
Reviewed By: CHW/DSJ
Approved By: TCW
JOB NO. 9610-001
FIG. 4
REV.
SSE - E.W. HORIZONTAL
2% DAMPING RESPONSE SPECTRA
S3 & S4 METHOD
IMPEDANCE METHOD
ISSUED
1.5
1.4
1.3
1.2
1.1
1.0
0.9
0.8
0.7
0.6
0.5
0.4
0.3
0.2
0.1
0
ACCELERATION (g's)
.225
.01
.02
.03
.04
.05
.06
.08
.1
.2
.3
.4
.5
.6
.8
1
2
3
4
5
PERIOD (seconds)

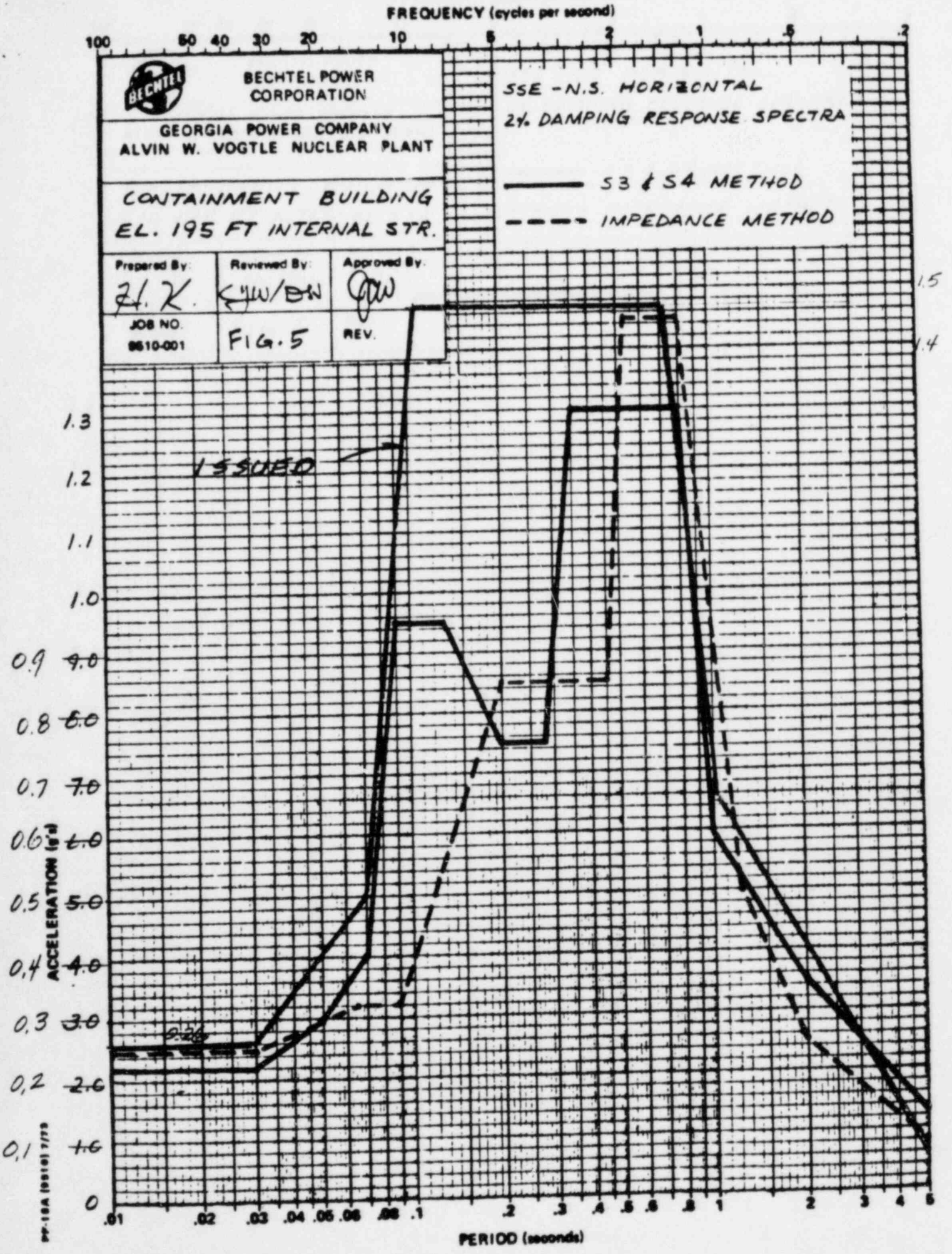
FREQUENCY (cycles per second)
100
50
40
30
20
10
5
2
1
.5
.2
BECHTEL POWER CORPORATION
GEORGIA POWER COMPANY
ALVIN W. VOGTLE NUCLEAR PLANT
CONTAINMENT BUILDING
EL. 195 FT INTERNAL STR.
Prepared By: Z.K.
Reviewed By: KJW/DN
Approved By: GJW
JOB NO. 9610-001
FIG. 5
REV.
SSE - N.S. HORIZONTAL
2% DAMPING RESPONSE SPECTRA
S3 & S4 METHOD
IMPEDANCE METHOD
ISSUED
1.5
1.4
1.3
1.2
1.1
1.0
0.9
0.8
0.7
0.6
0.5
0.4
0.3
0.2
0.1
0
9.0
8.0
7.0
6.0
5.0
4.0
3.0
2.6
1.6
ACCELERATION (g's)
.01
.02
.03
.04
.05
.06
.08
.1
.2
.3
.4
.5
.6
.8
1
2
3
4
5
PERIOD (seconds)

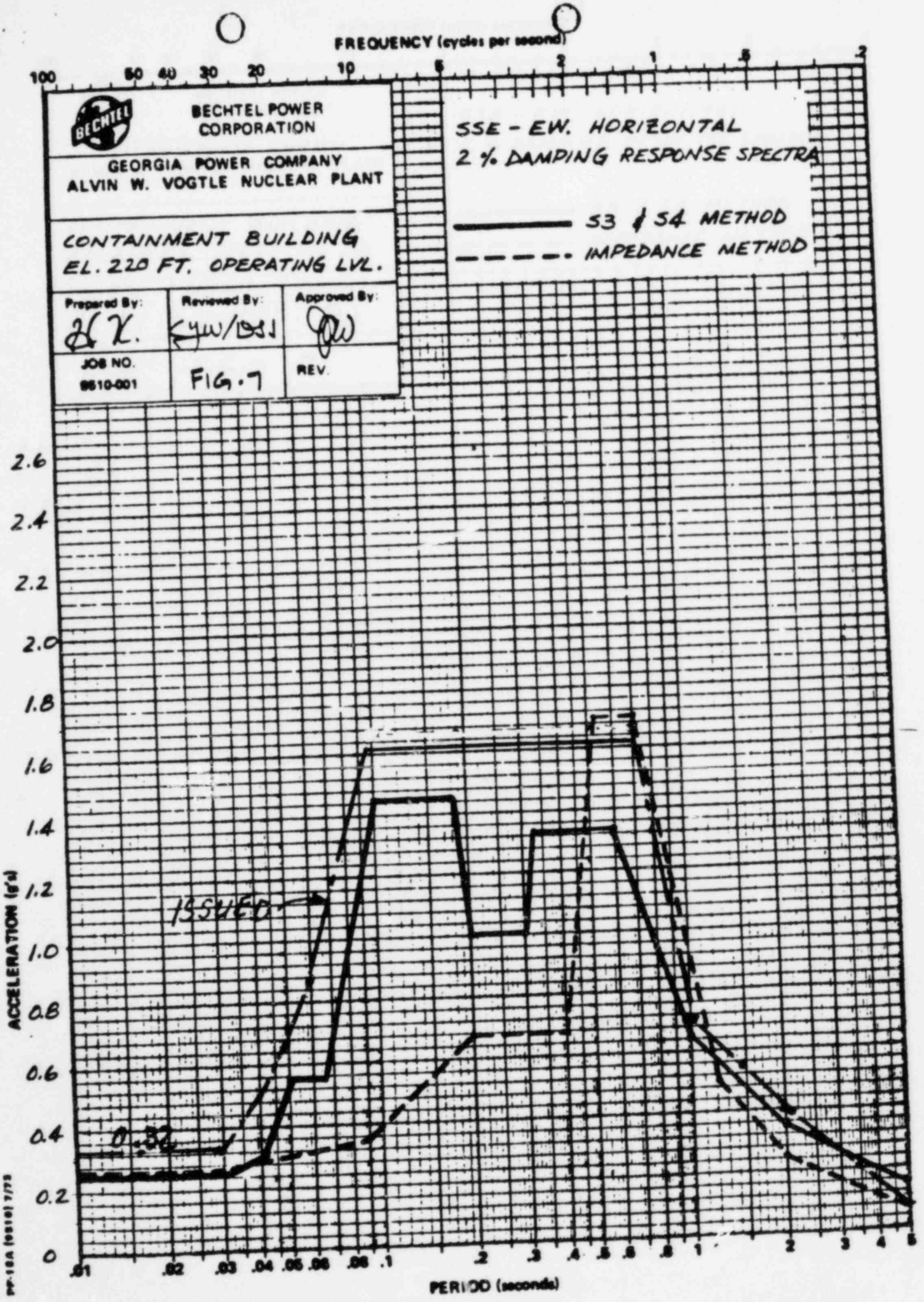
FREQUENCY (cycles per second)
100
50
40
30
20
10
5
2
1
.5
.2
BECHTEL POWER CORPORATION
GEORGIA POWER COMPANY
ALVIN W. VOGTLE NUCLEAR PLANT
CONTAINMENT BUILDING
EL. 220 FT. OPERATING LVL.
Prepared By:
Reviewed By:
Approved By:
JOB NO.
9610-001
FIG. 7
REV.
SSE - EW. HORIZONTAL
2 % DAMPING RESPONSE SPECTRA
S3 & S4 METHOD
IMPEDANCE METHOD
ISSUED
0.36
ACCELERATION (g's)
2.6
2.4
2.2
2.0
1.8
1.6
1.4
1.2
1.0
0.8
0.6
0.4
0.2
0
.01
.02
.03
.04
.05
.06
.08
.1
.2
.3
.4
.5
.6
.8
1
2
3
4
5
PERIOD (seconds)

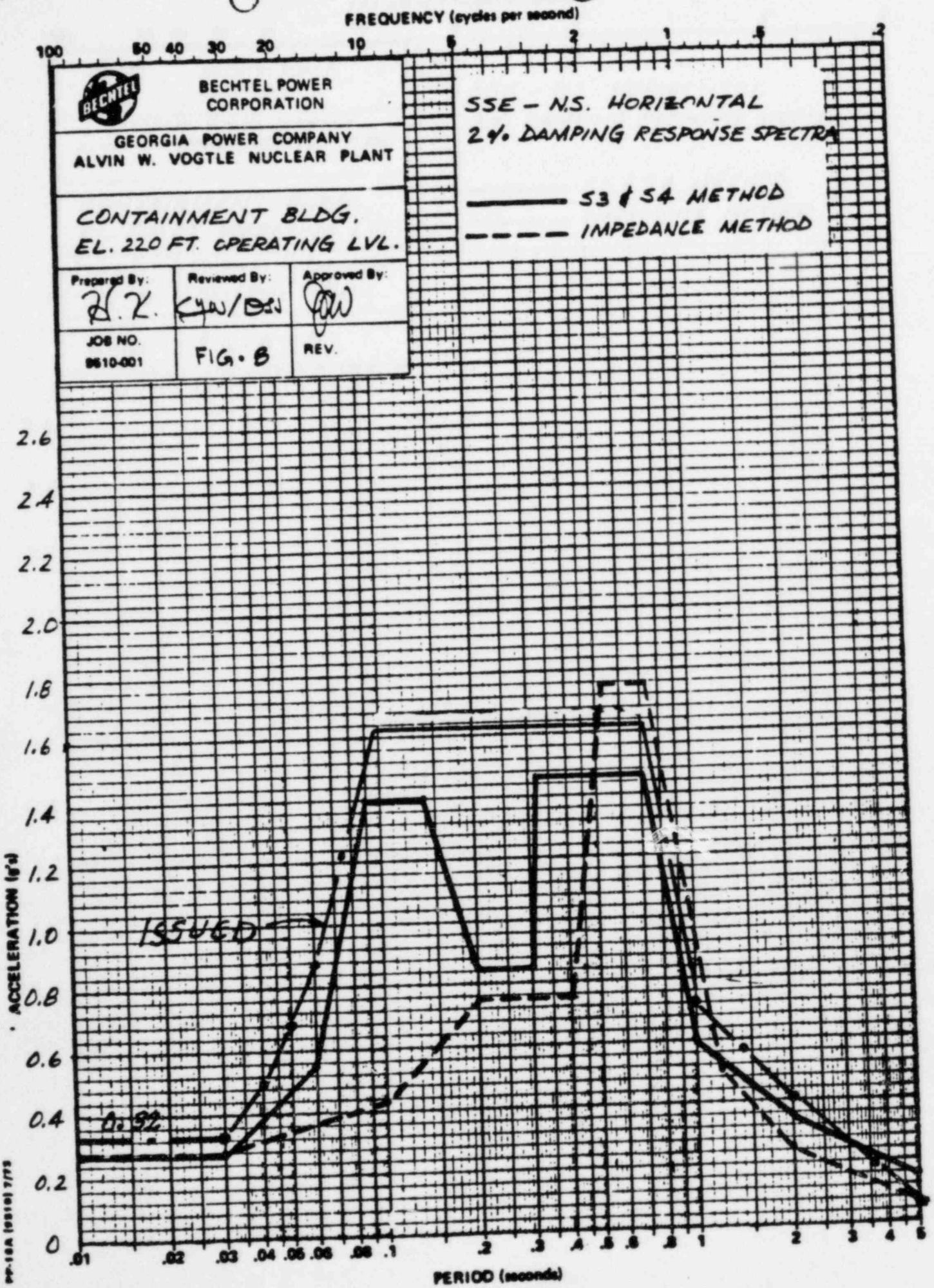
FREQUENCY (cycles per second)
100
50
40
30
20
10
5
2
1
.5
.2
BECHTEL POWER CORPORATION
GEORGIA POWER COMPANY
ALVIN W. VOGTLE NUCLEAR PLANT
CONTAINMENT BLDG.
EL. 220 FT. OPERATING LVL.
Prepared By:
Reviewed By:
Approved By:
JOB NO.
9610-001
FIG. 8
REV.
SSE - N.S. HORIZONTAL
2% DAMPING RESPONSE SPECTRA
S3 & S4 METHOD
IMPEDANCE METHOD
ISSUED
0.92
ACCELERATION (g's)
2.6
2.4
2.2
2.0
1.8
1.6
1.4
1.2
1.0
0.8
0.6
0.4
0.2
0
.01
.02
.03
.04
.05
.06
.08
.1
.2
.3
.4
.5
.6
.8
1
2
3
4
5
PERIOD (seconds)

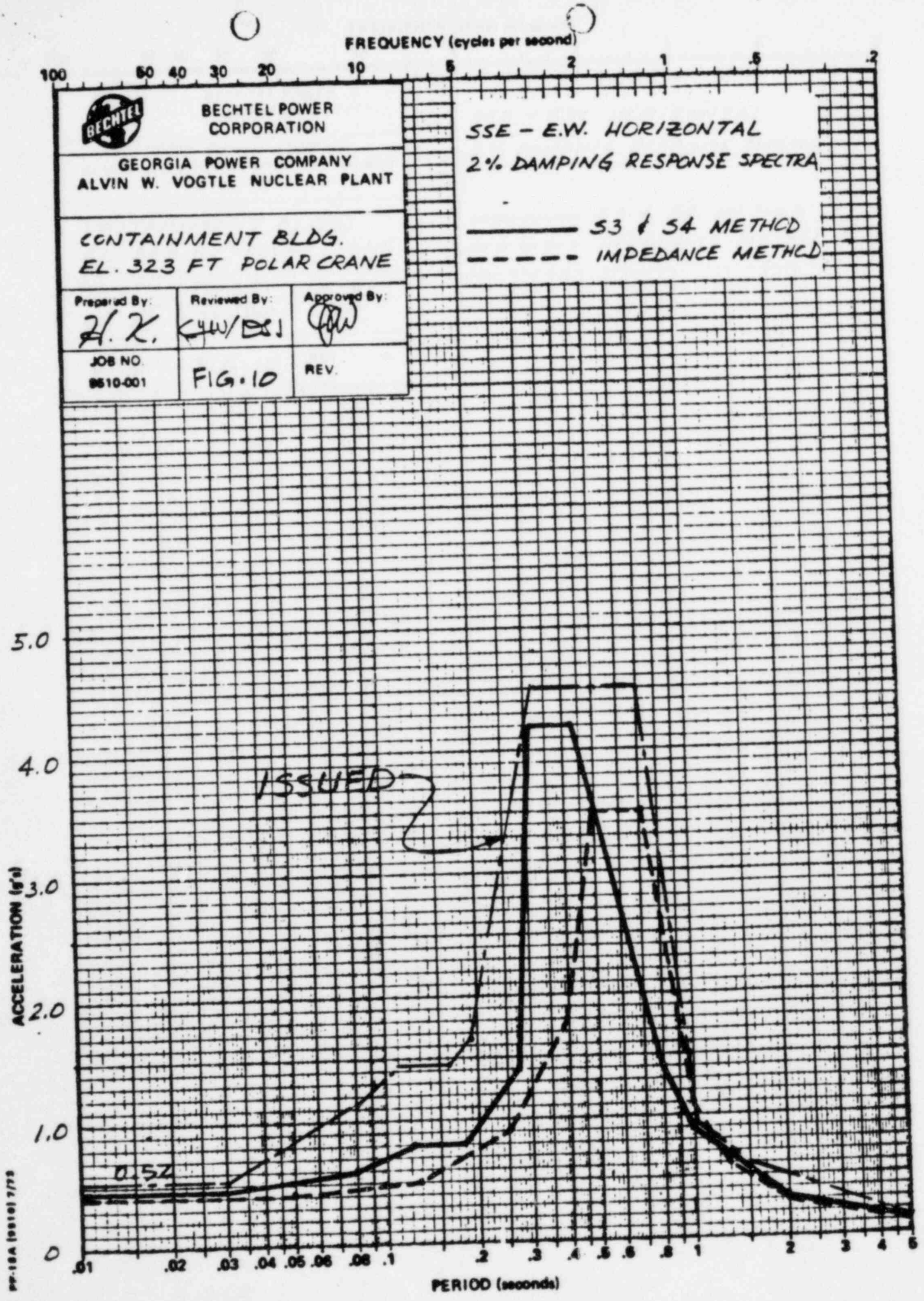
FREQUENCY (cycles per second)
100
50
40
30
20
10
5
2
1
.5
.2
BECHTEL POWER CORPORATION
GEORGIA POWER COMPANY
ALVIN W. VOGTLE NUCLEAR PLANT
CONTAINMENT BLDG.
EL. 323 FT POLAR CRANE
Prepared By: H. K.
Reviewed By: KJW/DCJ
Approved By:
JOB NO. 9510-001
FIG. 10
REV.
SSE - E.W. HORIZONTAL
2% DAMPING RESPONSE SPECTRA
S3 & S4 METHOD
IMPEDANCE METHOD
ISSUED
5.0
4.0
3.0
2.0
1.0
0
ACCELERATION (g's)
0.52
.01
.02
.03
.04
.05
.06
.08
.1
.2
.3
.4
.5
.6
.8
1
2
3
4
5
PERIOD (seconds)

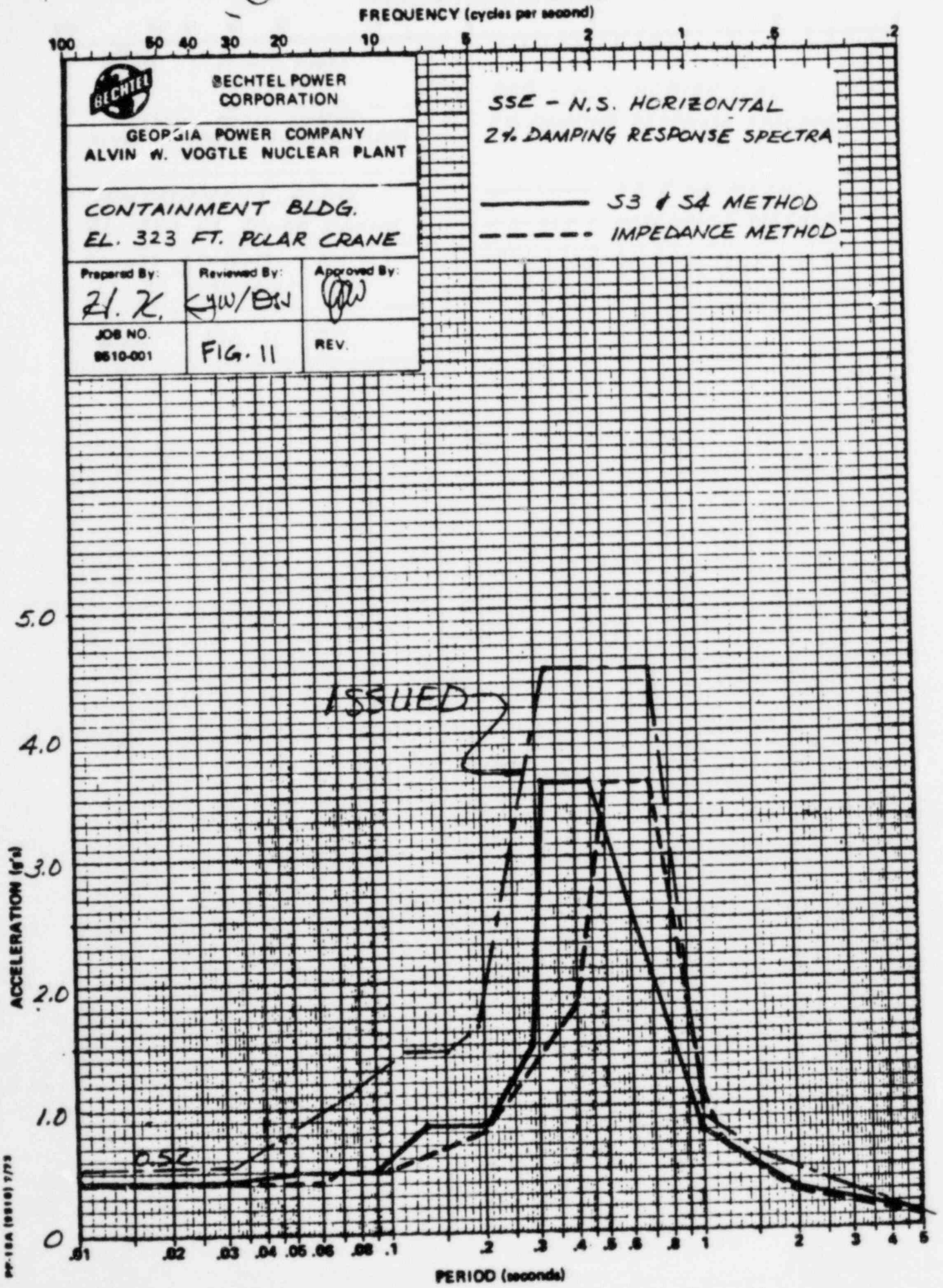
FREQUENCY (cycles per second)
100
50
40
30
20
10
5
2
1
.5
.2
BECHTEL POWER CORPORATION
GEORGIA POWER COMPANY
ALVIN W. VOGTLE NUCLEAR PLANT
CONTAINMENT BLDG.
EL. 323 FT. POLAR CRANE
Prepared By: H. K.
Reviewed By: KJW/BJN
Approved By: KJW
JOB NO. 9510-001
FIG. 11
REV.
SSE - N.S. HORIZONTAL
2% DAMPING RESPONSE SPECTRA
S3 & S4 METHOD
IMPEDANCE METHOD
ISSUED
5.0
4.0
3.0
2.0
1.0
0
ACCELERATION (g's)
0.5Z
.01
.02
.03
.04
.05
.06
.08
.1
.2
.3
.4
.5
.6
.8
1
2
3
4
5
PERIOD (seconds)

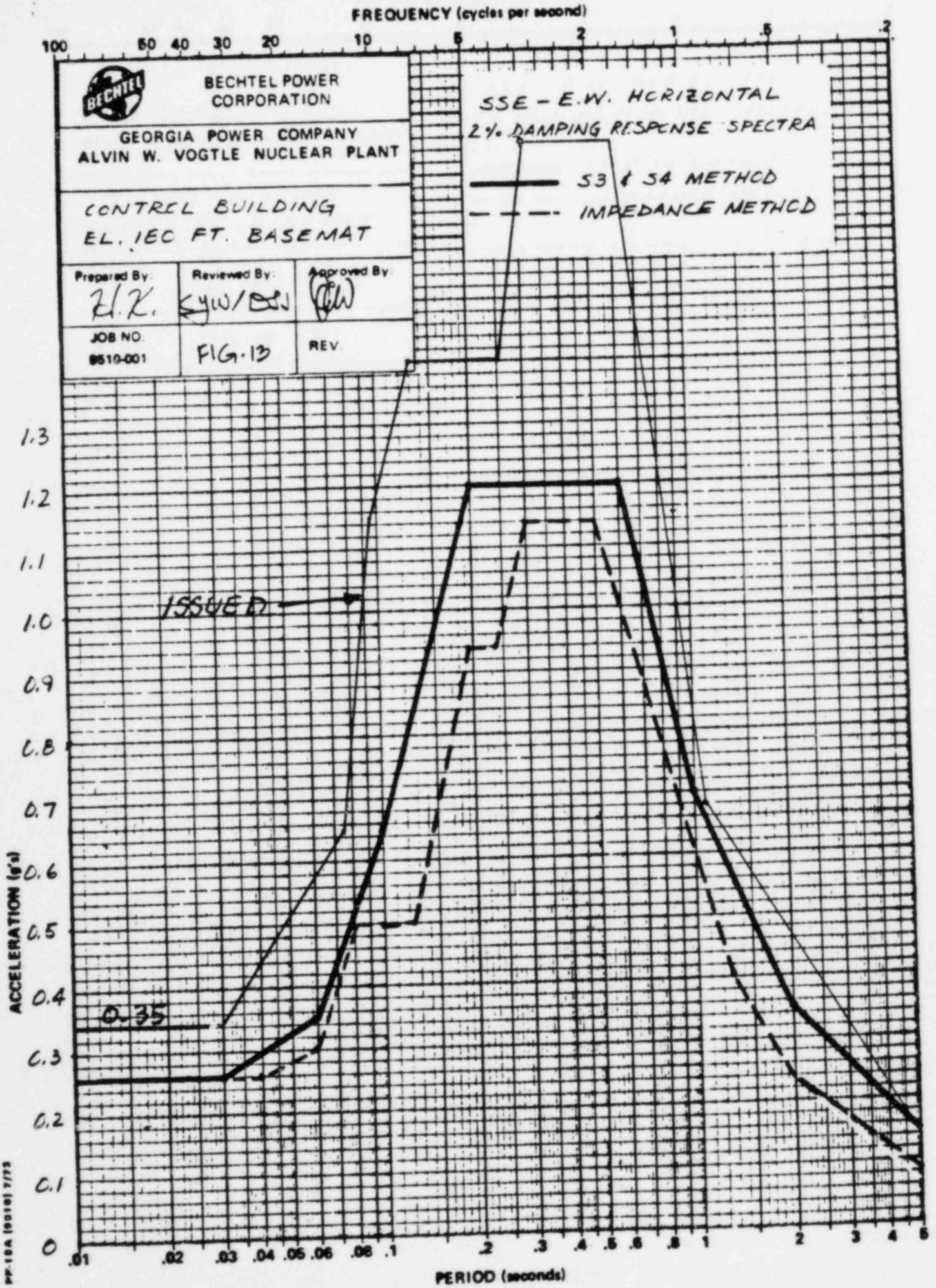
FREQUENCY (cycles per second)
100 50 40 30 20 10 5 2 1 .5 .2
BECHTEL POWER CORPORATION
GEORGIA POWER COMPANY
ALVIN W. VOGTLE NUCLEAR PLANT
CONTROL BUILDING
EL. 160 FT. BASEMAT
Prepared By: H.K.
Reviewed By: KYW/DSJ
Approved By: (illegible)
JOB NO. 9610-001
FIG. 13
REV.
SSE - E.W. HORIZONTAL
2% DAMPING RESPONSE SPECTRA
S3 & S4 METHOD
IMPEDANCE METHOD
ISSUED
0.35
ACCELERATION (g's)
1.3 1.2 1.1 1.0 0.9 0.8 0.7 0.6 0.5 0.4 0.3 0.2 0.1 0
.01 .02 .03 .04 .05 .06 .08 .1 .2 .3 .4 .5 .6 .8 1 2 3 4 5
PERIOD (seconds)

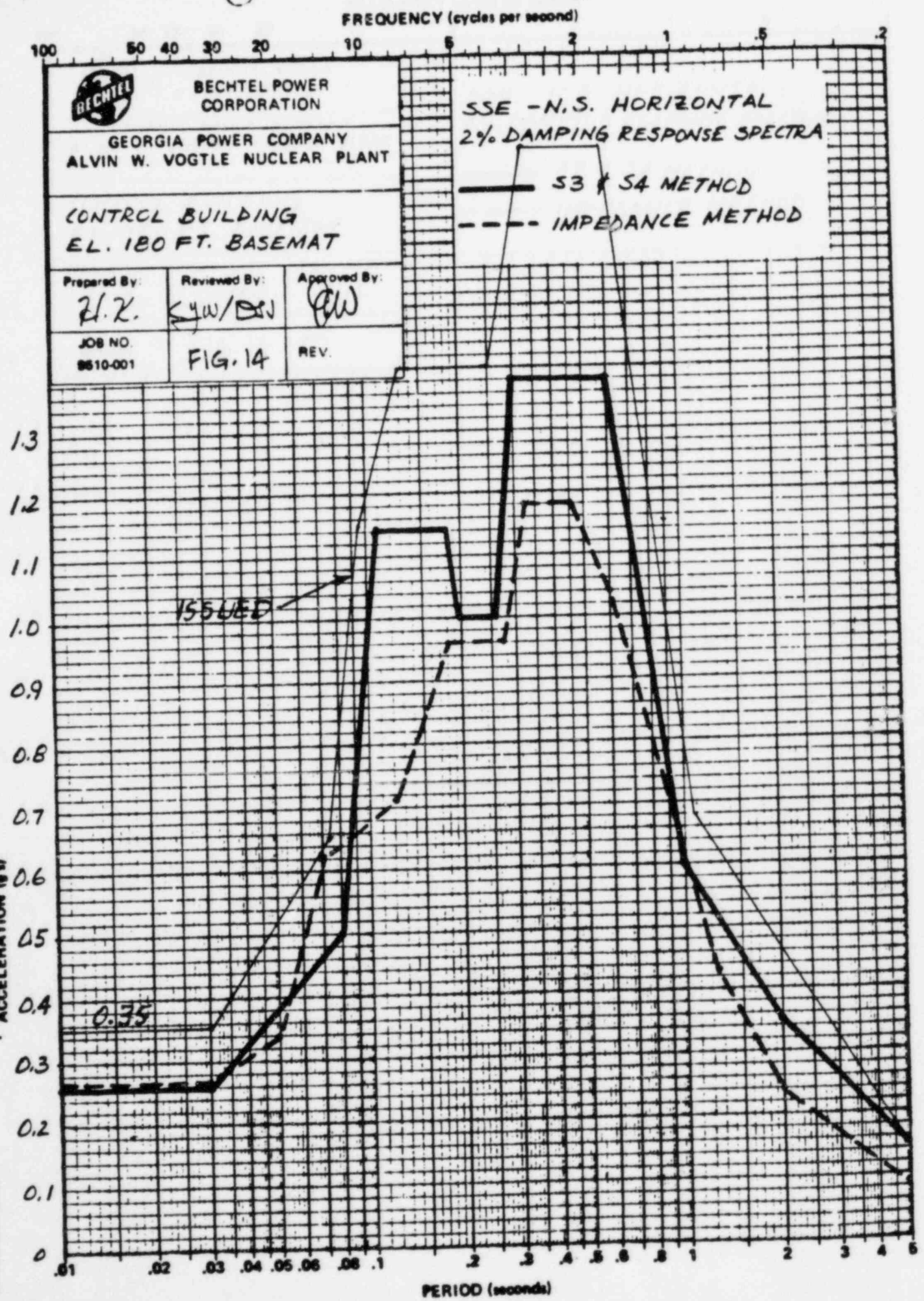
FREQUENCY (cycles per second)
100
50
40
30
20
10
5
2
1
.5
.2
BECHTEL POWER CORPORATION
GEORGIA POWER COMPANY
ALVIN W. VOGTLE NUCLEAR PLANT
CONTROL BUILDING
EL. 180 FT. BASEMAT
Prepared By: H.K.
Reviewed By: KJW/DSJ
Approved By: RW
JOB NO. 8610-001
FIG. 14
REV.
SSE - N.S. HORIZONTAL
2% DAMPING RESPONSE SPECTRA
S3 & S4 METHOD
IMPEDANCE METHOD
ISSUED
0.35
ACCELERATION (g's)
1.3
1.2
1.1
1.0
0.9
0.8
0.7
0.6
0.5
0.4
0.3
0.2
0.1
0
.01
.02
.03
.04
.05
.06
.08
.1
.2
.3
.4
.5
.6
.8
1
2
3
4
5
PERIOD (seconds)

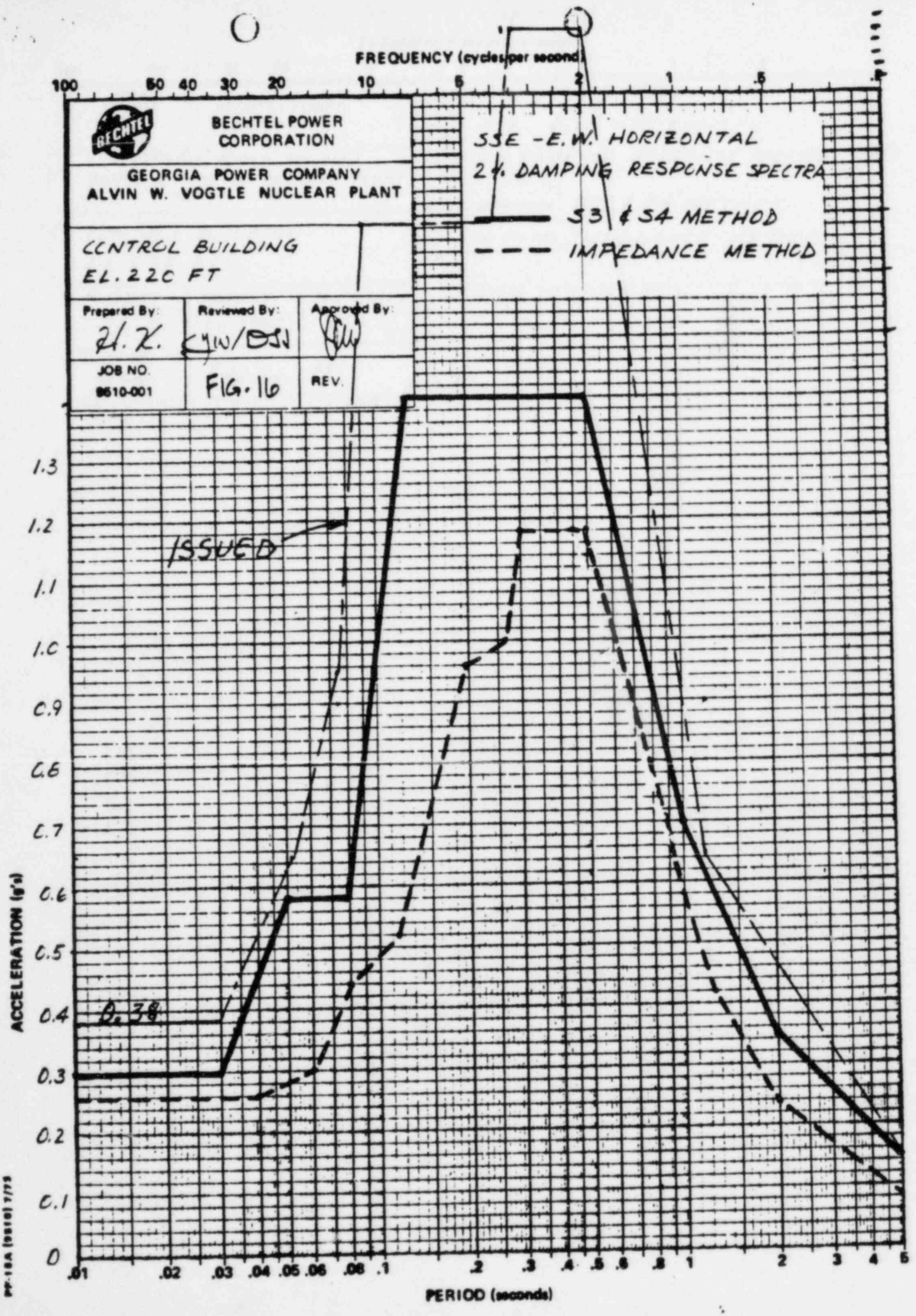
FREQUENCY (cycles per second)
100 50 40 30 20 10 5 2 1 .5
BECHTEL POWER CORPORATION
GEORGIA POWER COMPANY
ALVIN W. VOGTLE NUCLEAR PLANT
CONTROL BUILDING
EL. 220 FT
Prepared By: R. K.
Reviewed By: KJW/DSJ
Approved By:
JOB NO. 9610-001
FIG. 16
REV.
SSE - E.W. HORIZONTAL
2% DAMPING RESPONSE SPECTRA
S3 & S4 METHOD
IMPEDANCE METHOD
ISSUED
0.38
ACCELERATION (g's)
1.3 1.2 1.1 1.0 0.9 0.8 0.7 0.6 0.5 0.4 0.3 0.2 0.1 0
.01 .02 .03 .04 .05 .06 .08 .1 .2 .3 .4 .5 .6 .8 1 2 3 4 5
PERIOD (seconds)

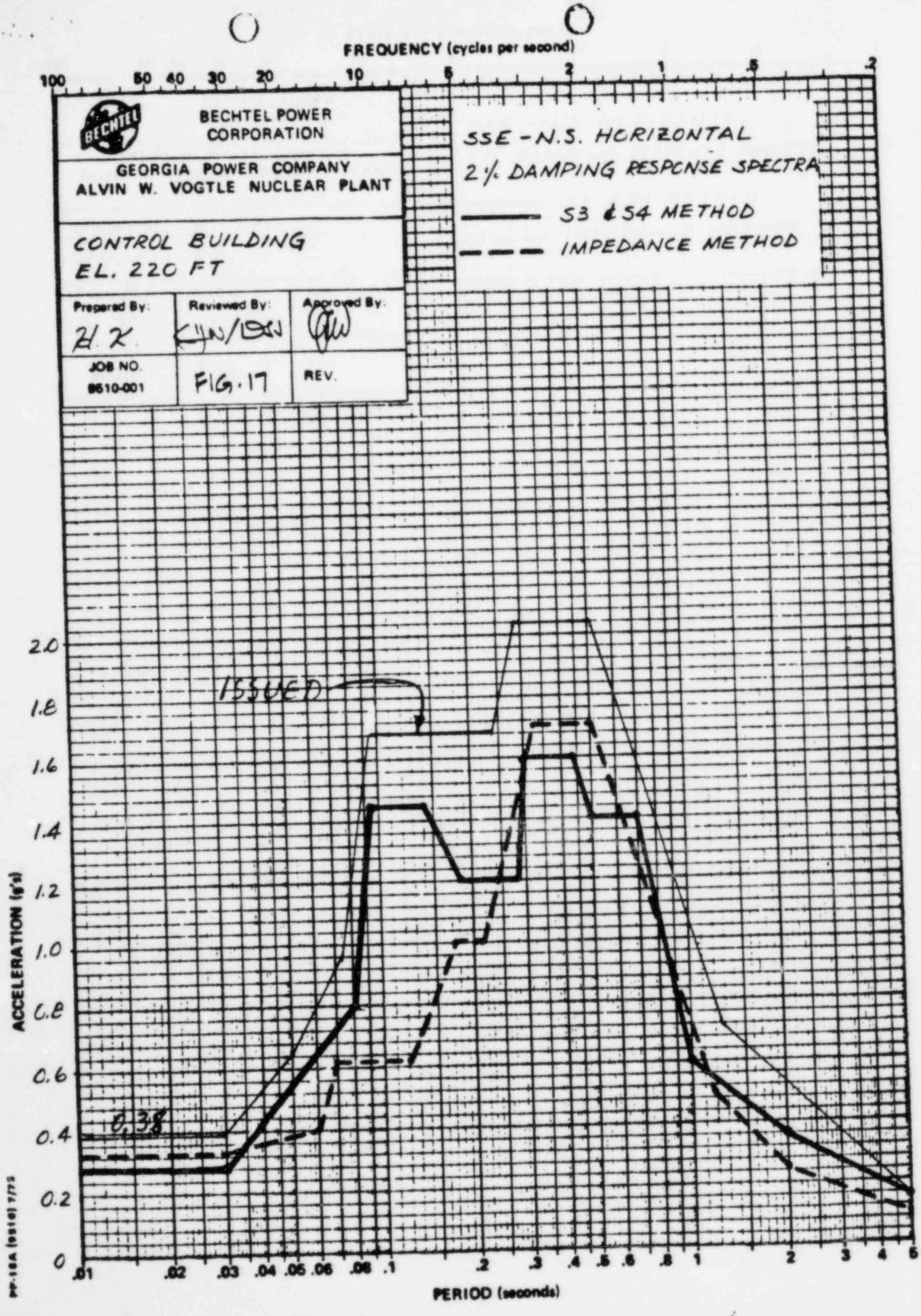
FREQUENCY (cycles per second)
100 50 40 30 20 10 5 2 1 .5 .2
BECHTEL POWER CORPORATION
GEORGIA POWER COMPANY
ALVIN W. VOGTLE NUCLEAR PLANT
CONTROL BUILDING
EL. 220 FT
Prepared By: H.K.
Reviewed By: KJN/DCN
Approved By:
JOB NO. 8610-001
FIG. 17
REV.
SSE - N.S. HORIZONTAL
2% DAMPING RESPONSE SPECTRA
S3 & S4 METHOD
IMPEDANCE METHOD
ISSUED
0.38
ACCELERATION (g's)
2.0
1.8
1.6
1.4
1.2
1.0
0.8
0.6
0.4
0.2
0
.01 .02 .03 .04 .05 .06 .08 .1 .2 .3 .4 .5 .6 .8 1 2 3 4 5
PERIOD (seconds)

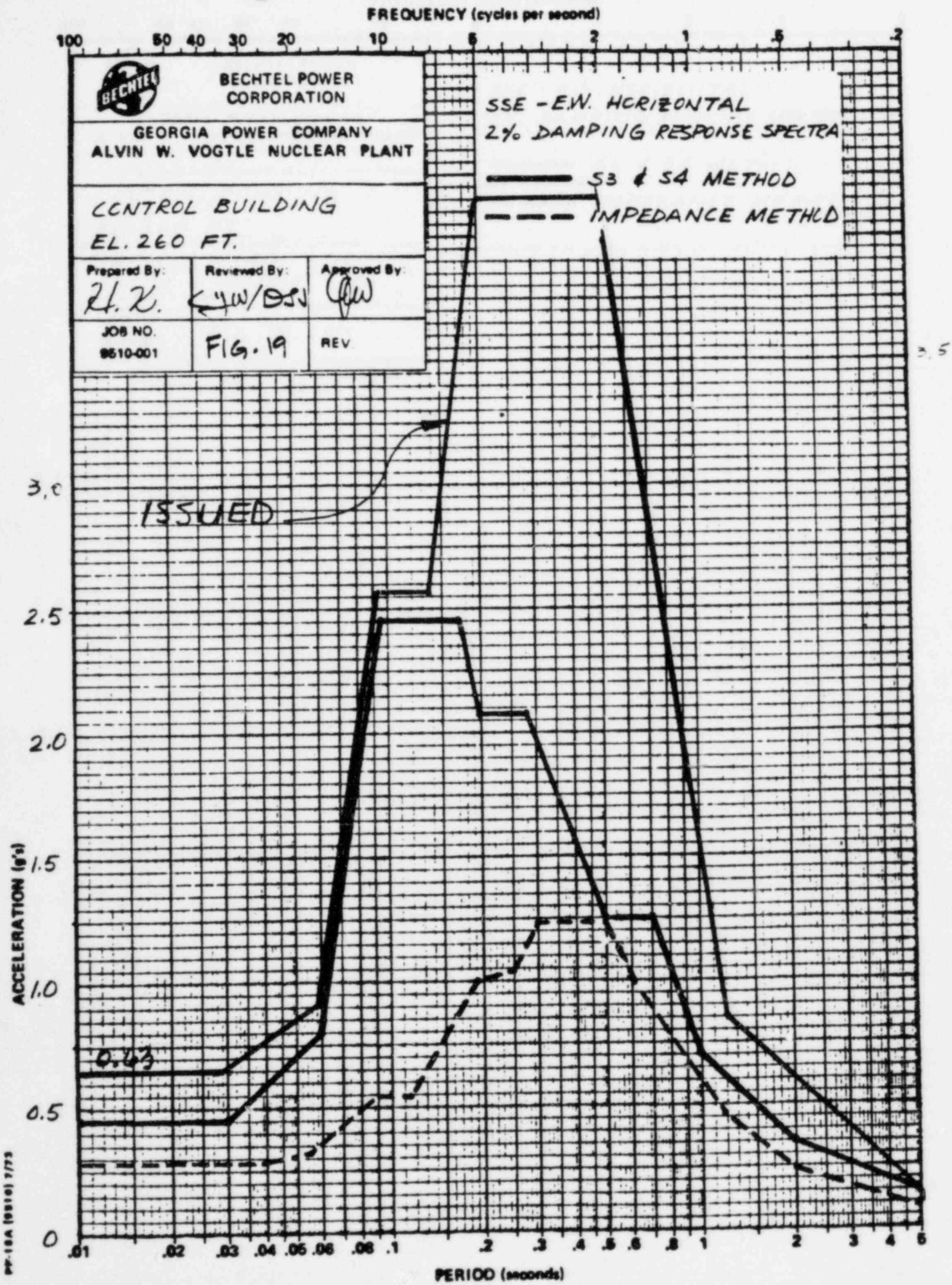
FREQUENCY (cycles per second)
100 50 40 30 20 10 5 2 1 .5 .2
BECHTEL POWER CORPORATION
GEORGIA POWER COMPANY
ALVIN W. VOGTLE NUCLEAR PLANT
CONTROL BUILDING
EL. 260 FT.
Prepared By: R.K.
Reviewed By: JW/DSJ
Approved By: JW
JOB NO. 9610-001
FIG. 19
REV
SSE - E.W. HORIZONTAL
2% DAMPING RESPONSE SPECTRA
S3 & S4 METHOD
IMPEDANCE METHOD
ISSUED
3.5
3.0
2.5
2.0
1.5
1.0
0.5
0
0.63
ACCELERATION (g's)
.01 .02 .03 .04 .05 .06 .08 .1 .2 .3 .4 .5 .6 .8 1 2 3 4 5
PERIOD (seconds)
PP-16A (9810) 7/73

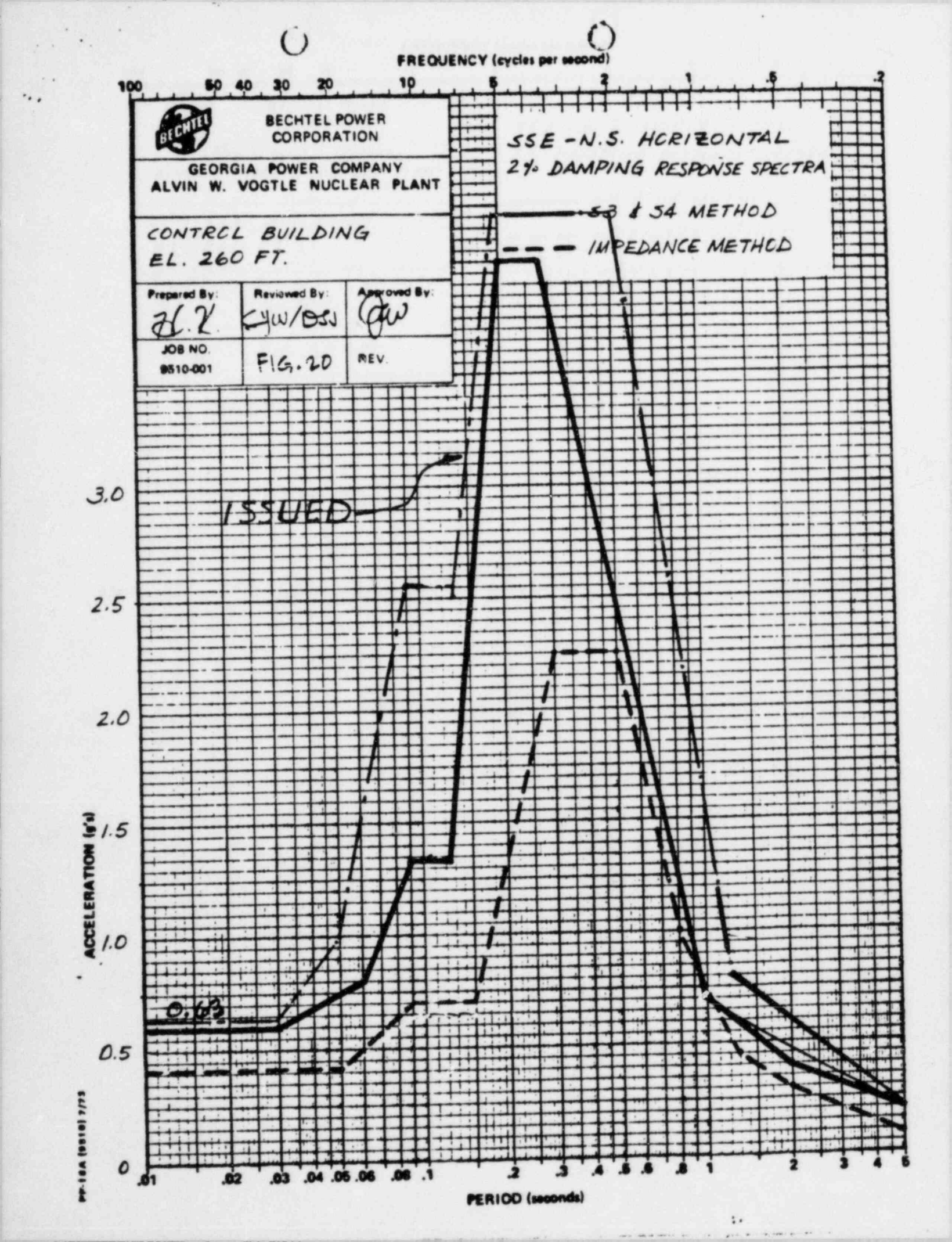
FREQUENCY (cycles per second)
100
50
40
30
20
10
5
2
1
.5
.2
BECHTEL POWER CORPORATION
GEORGIA POWER COMPANY
ALVIN W. VOGTLE NUCLEAR PLANT
CONTROL BUILDING
EL. 260 FT.
Prepared By:
Reviewed By:
Approved By:
JOB NO.
9510-001
FIG. 20
REV.
SSE - N.S. HORIZONTAL
2% DAMPING RESPONSE SPECTRA
S3 & S4 METHOD
IMPEDANCE METHOD
ISSUED
3.0
2.5
2.0
1.5
1.0
0.5
0
ACCELERATION (g's)
0.03
.01
.02
.03
.04
.05
.06
.08
.1
.2
.3
.4
.5
.6
.8
1
2
3
4
5
PERIOD (seconds)

Enclosure 4

STRUCTURAL AUDIT MEETING FOR VOGTLE

ACTION ITEMS

1. Include as part of the FSAR, Appendix 3D, all items of the November 13, 1978 GPC letter to the NRC (confirmatory study, sensitivity study, and methodology to account for torsion caused by the seismic wave propagation effects). In addition, include therein a comparison of the VEGP design in-structure response spectra (e.g., envelope of N-S and E-W response spectra considered applicable for any two mutually orthogonal horizontal directions) with the response spectra provided in the confirmatory study, and the resulting conclusions.

2. Provide justification for using the component factor method (1.0, 0.4, 0.4) in lieu of the square root of the sum of the squares (SRSS) method for consideration of three component earthquake effects.

3. Provide the basis for the equation used in determining the rotational mass moment of inertia in the containment model.

4. Provide the basis for concluding that, for the containment basemat design, the combination including 100 percent of the vertical seismic loads in the component factor method does not control over the other combinations including 100 percent of the seismic loads in either horizontal direction.

5. Provide justification for the use of 25 percent of the design live load in the containment internal structure design for the load combination involving earthquake load effects. Provide similar justification for the control building basemat.

6. Select the worst case for the contaiment internal structure steel beam-to-column connections and demonstrate the adequacy of the connection and column design considering the moment resistance introduced by the connecting gussets.

7. Provide the basis for the conclusion that the OBE loading combination governs the design of slabs in the auxiliary building, rather than the SSE condition.

8. Check the effect of tornado depressurization on the Category I tank wall together with hydrostatic pressure.

BECHTEL POWER CORPORATION

SEISMIC COMMITTEE

NEWSLETTER NO. 6

July 1, 1976

SUBJECT: Combination Of Co-directional Responses Due To Three Earthquake Input Components By The Component Factor Method.

SUMMARY: Let R_i, R_j, and R_k be the three maximum co-directional responses resulting separately from the three earthquake input components in the i, j, and k directions respectively. Presently, these are combined by the method of the square root of the sum of the squares (SRSS) because of the unlikelihood of their simultaneous occurrence.

Thus:

$$R = \text{Combined Response} = \sqrt{R_i^2 + R_j^2 + R_k^2} \qquad (1)$$

The SRSS method has an inherent difficulty for certain engineering applications such as the design of base mats where separation of the base from the soil is anticipated. Under such circumstances, the alternative is to consider an equivalent set of three simultaneously occurring maxima, R_i, $0.4R_j$, and $0.4R_k$, such that

$$R = R_i + 0.4R_j + 0.4R_k \qquad (2)$$

where $R_i \geq R_j$ and R_k.

The following discussion verifies the adequacy of Eq. (2). Its probable maximum error with respect to the SRSS method is less than 1%.

DISCUSSION: To establish the adequacy of the factor method expressed by Eq. (2), first consider a combined response, R', defined below:

$$R' = R_i + 0.414R_j + 0.318R_k \tag{3}$$

in which

$$R_i \geq R_j \geq R_k \tag{4}$$

Let

$$R_j = \bar{R}_j + R_k \qquad (\bar{R}_j = 0 \text{ if } R_j = R_k)$$

$$R_i = \bar{R}_i + R_j = \bar{R}_i + \bar{R}_j + R_k \qquad (\bar{R}_i = 0 \text{ if } R_i = R_j) \tag{5}$$

According to Eq. (1), the SRSS method gives:

$$R = \{(\bar{R}_i + \bar{R}_j + R_k)^2 + (\bar{R}_j + R_k)^2 + R_k^2\}^{1/2}$$

$$= \{3R_k^2 + 2\bar{R}_j^2 + \bar{R}_i^2 + 2\bar{R}_i(\bar{R}_j + R_k) + 4\bar{R}_j R_k\}^{1/2} \tag{6}$$

According to Eq. (3),

$$R' = (\bar{R}_i + \bar{R}_j + R_k) + 0.414(\bar{R}_j + R_k) + 0.318R_k$$

$$= 1.732R_k + 1.414\bar{R}_j + \bar{R}_i = \{[1.732R_k + 1.414\bar{R}_j + \bar{R}_i]^2\}^{1/2}$$

$$= \{3R_k^2 + 2\bar{R}_j^2 + \bar{R}_i^2 + 2\bar{R}_i(1.414\bar{R}_j + 1.732R_k) + 4.9\bar{R}_j R_k\}^{1/2} \tag{7}$$

Comparing Eqs. (6) and (7), it is obvious that the combined response calculated according to Eq. (3) is always more conservative than the combined response by the SRSS method. In the special case that $R_i = R_j = R_k$, they become identical to each other, i.e., $R = R' = \sqrt{3}R_k$.

For convenience of engineering applications, Eq. (3) can be simplified by replacing the factors 0.414 and 0.318 by a common factor of 0.4. This reduces Eq. (3) to Eq. (2). By inspection, the maximum probable error of Eq. (2) with respect to the SRSS method is less than 1%. This maximum error occurs when $R_k = 0$ and $R_i = R_j$. In this special case, the SRSS method gives $R = 1.41R_i$ and Eq. (2) gives $R = 1.4R_i$.

INTERNATIONAL SYMPOSIUM ON
EARTHQUAKE STRUCTURAL ENGINEERING
St. Louis, Missouri, USA, August, 1976

DISCRETE MODELING OF SYMMETRIC BOX-TYPE STRUCTURES

A. H. HADJIAN AND T. S. ATALIK

Engineering Specialist and Engineer

Bechtel Power Corporation, Los Angeles Division

Norwalk, California, U.S.A.

SUMMARY

The dynamic modeling of box-type structures with simple lumped mass models is evaluated. Shear deformations, rotatory inertia and shear lag effects have important contributions to the overall response depending on the characteristics of the structure. To routinely incorporate these effect, a simplified procedure is described. The effects of shear deformation and rotatory inertia effects on the mass properties of the structure are accounted for by heuristically reducing the consistant mass matrix of a beam element into a diagonal form. These effects are then isolated and checked against the analytical solutions with acceptable results. The incorporation of shear lag effects is approached from a statics point of view. Based on a bending theory developed by Reisner, the stiffness of the beam is modified such that the use of the elementary bending theory would correctly predict deflections of beams with significant shear lag effects. The effect of shear lag on the inertial properties is investigated only by a few test cases. The procedure developed is tested by a comparison of the results with those from a finite element model of a structure whose properties were intentionally selected such as to accentuate the considerations under investigation.

INTRODUCTION

It is common engineering practice to use simplified lumped mass models in predicting the dynamic characteristics and earthquake response of structures. For complicated structures, such as those encountered in nuclear power plants, a finite element model could, in principle, provide a more appropriate representation. However, due to the associated high computer costs, lengthy modeling labor, the non-availability of large problem solving capabilities and the uncertainties in the other aspect of the problem, it is usually deemed adequate that a simplified lumped mass model would represent the dynamic characteristics of these relatively complicated structures. However, it is important that a) the modeling techniques used be first qualified using simpler structures, b) these simpler structures be studied to identify the important parameters of the modeling process, and c) based on the above two steps, modeling techniques for the more complicated structures be formulated. The first two steps are the subject of this paper. A subsequent paper will deal with the third phase.

The following areas are considered to be particularly important for the modeling of box-type concrete structures: a) The proper location of the shear center. b) The determination of the effective shear area. c) Shear lag effects in the computation of moment of inertias. d) The lumping of mass and of rotatory inertia at selected nodes and the effects of shear deformation on the mass matrix. e) The possible effects of shear lag and effective shear area on the inertial masses.

SHEAR CENTER OF RESISTING ELEMENTS

The shear center is the point through which a transverse loading will not cause any twisting of the cross-section. Although equations for the calculation of the shear center for open sections are available in texts on advanced strength of materials (6), those for closed sections are more difficult to obtain (7). More importantly the application of these concepts to complicated floor plans encountered in nuclear power plant structures is not a trivial task. It is common practice though to calculate instead the center of rigidity in each of the "principal" structure axes by considering only the walls parallel to the direction under consideration. Obviously for an open channel section such as shown in Fig. 1a, this assumption is not justified. Fig. 1b shows an unsymmetrical box where the assumption of the center of rigidity as defined above, is seen to be a very good approximation to the true shear center. A more detailed study of this approximation is in order for more complicated structures; however, such a study is beyond the scope of the present paper. It is obvious that for sections having two axes of symmetry, the shear center and the centroid of the section coincide.

EFFECTIVE SHEAR AREA

In the derivation of the Timoshenko beam equation the effective shear area is introduced to account for the fact that shear stress and shear strain are not uniformly distributed over the cross-section. Although there are many interpretations to the actual meaning of the shear coefficient, K, (1, 2, or 3), the important point to note is that except for Timoshenko's (8), the differences in the actual values are of no significant importance in practical applications in earthquake engineering. Although

the equations for
ratio, ν, the diff
is not significant
In the present pap
and Billington (2)
of these shear coe
intent of such a c
Ebner and Billingt
apply to more comp

A further sim
cross-section to t
based on Cowper's
with the Cowper re
results indicate t
section breaks dow
conclusion is base
box could not be l
independent rectan
the shear area coe
when used will be

SHEAR LAG EFFECTS

Considering b
that the normal st
of bending) does n
the flanges this a
problem is illustr
bending about the
sections remain pl
effect reducing th
wise been calculat
ing, a method of o
including shear la

Using the pri
the following gove
when the shear lag

$$Z''$$

$$U''$$

with the boundary

$$U = 0$$

$$U' +$$

the equations for K as reported by Cowper (1) are dependent on Poisson's ratio, ν, the differences between the range of ν commonly used for concrete is not significant at all. Thus a value of ν = .17 is used in this paper. In the present paper both Cowper's equations (1) and that given by Ebner and Billington (2) will be used; however, a direct dimensionless comparison of these shear coefficients will not be attempted in this paper. The intent of such a comparison would be to establish the generality of the Ebner and Billington equation, since it could most suitably be extended to apply to more complicated sections.

A further simplification would be to relate the shear area of the cross-section to the area of the "webs" only. Results of such an attempt, based on Cowper's equation for a box section, are shown in Fig. 2, togeth r with the Cowper results. The variables are explained in the figure. These results indicate that the generality of the Cowper equation for the box section breaks down for certain values of M and N (dashed lines). This conclusion is based on the observation that the shear area of the complete box could not be less than that of the shear area of the webs treated as independent rectangular sections. For ν = 0.17, the Cowper equation gives the shear area coefficient for rectangles as 0.844. The Cowper equation when used will be limited as discussed above.

SHEAR LAG EFFECTS IN BENDING STIFFNESS

Considering bending stiffness only, the elementary beam theory assumes that the normal stress along the flanges (the walls normal to the direction of bending) does not vary. However, because of the shear deformation of the flanges this assumption often leads to errors for wide beams. The problem is illustrated schematically in Fig. 3. For the section shown, bending about the Y-axis would rotate the web of the section assuming plane sections remain plane. However, the flanges would deform as shown; thus in effect reducing the moment of inertia of the section as would have otherwise been calculated according to the elementary beam theory. In the following, a method of obtaining an effective moment of inertia of box sections including shear lag effects is presented.

Using the principle of minimum potential energy Reissner (5) developed the following governing equations for the deflection of a box beam (Fig. 4) when the shear lag effects are present:

$$Z'' + \frac{2}{3}\,\frac{I_f}{I}\,U' + \frac{M}{EI} = 0 \tag{1}$$

$$U'' - \frac{5}{2}\,\frac{G}{E}\,\frac{U}{w^2} + \frac{5}{4}\,Z''' = 0 \tag{2}$$

with the boundary conditions

$$\begin{aligned} &U = 0, \text{ at a section where the flange is fixed} \\ &U' + \frac{5}{4}\,Z'' = 0, \text{ at a section where the flange is free} \end{aligned} \tag{3}$$

In the above equations Z is the transverse deflection, $I_f = 4wth^2$ is the moment of inertia of the flanges, $I_w = 4bh^3/3$ is the moment of inertia of the webs, $I = I_w + I_f$ is the total moment of inertia of the cross-section, M is the moment at the section, E and G are Young's modulus and shear modulus respectively, U = U(x) is a function denoting the magnitude of the shear lag effects and it is assumed that the spanwise flange deformation u(x,y) may be approximated by

$$u(x,y) = \pm h \left[Z' + \left(1 - \frac{y^2}{w^2}\right) U(x) \right] \tag{4}$$

Herein, prime denotes differentiation with respect to the spatial variable x. The variables w, t, h and b describe the dimensions of the cross-section as depicted in Fig. 4.

Differentiating Eqn. 1 once and back substituting into Eqn. 2 one gets a differential equation for the shear lag function U as

$$U'' - k^2 U = \frac{5}{4} n \frac{M'}{EI} \tag{5}$$

with the boundary conditions

$$U = 0, \text{ at the fixed end} \tag{6}$$

$$U' = \frac{5}{4} n \frac{M}{EI}, \text{ at the free end} \tag{7}$$

where $k = \frac{1}{w}\sqrt{\frac{5nG}{2E}}$ and $n = \frac{1}{1 - 5I_f/6I}$ (8)

Once the shear lag function U is found for a specific case from Eqn. 5, the static deflection of the box beam can be solved by a double integration of Eqn. 1 with the appropriate boundary conditions,

$$Z'' = -\frac{M}{EI} - \frac{2}{3}\frac{I_f}{I} U' \tag{9}$$

Since the aim is to obtain a reduction factor for the flange stiffnesses a further simplification of Eqn. 9 is necessary. This can be achieved as follows: For a given moment variation, M = M(x), solve for U = U(x) from Eqns. 5, 6 and 7. Find the constant 'a' such that

$$U'(x) \cong a \cdot M(x) \tag{10}$$

Herein the constant 'a' is found by minimizing the average over the length, of the square of the difference between U'(x) and a · M(x); that is

$$H = \int_0^{\ell} [U'(x) - aM(x)]^2 \, dx \quad \text{minimum} \tag{11}$$

ion, $I_f = 4wth^2$ is
e moment of inertia
of the cross-section,
ılus and shear modulus
tude of the shear lag
rmation u(x,y) may

(4)

to the spatial
mensions of the

nto Eqn. 2 one gets

(5)

(6)

(7)

(8)

ic case from Eqn. 5,
double integration

(9)

e flange stiffnesses
n be achieved as
or U = U(x) from

(10)

verage over the
a · M(x); that is

minimum (11)

or
$$\frac{\partial H}{\partial a} = 0 \Rightarrow a = \frac{\int_0^{\ell} U'(x).M(x)dx}{\int_0^{\ell} M^2(x)dx} \tag{12}$$

Back substituting the approximation to U' into Eqn. 9 gives

$$Z'' = -\frac{M}{EI} - \frac{2}{3}\frac{I_f}{I}(aM) \tag{13}$$

or
$$Z'' = -\frac{M}{EI}\left(1 + \frac{2}{3}EI_f\, a\right) \tag{14}$$

The expression within the parenthesis in Eqn. 14 is the factor by which the simple beam deflection field is to be modified to include the effects of shear lag.

To find the reduction factor of the flange stiffness due to shear lag, let

$$\alpha = 1 + \frac{2}{3}EI_f\, a \tag{15}$$

then find β such that

$$\frac{\alpha}{I} = \frac{1}{I_w + \beta I_f} \tag{16}$$

Solving for β one obtains

$$\beta = I/\alpha I_f - I/I_f + 1 \tag{17}$$

The variable β defined in Eqn. 17 may be interpreted as the flange stiffness reduction factor due to shear lag effects.

The changes in β as a function of the ratio of beam length to half flange width for three different loading conditions, namely, an end point load, a uniformly distributed load and a triangular load are given in Figures 5 through 7. Table 1 shows the maximum error in the displacements of typical box-beams, for each of the three loading conditions, when the shear lag effects are introduced approximately using the present approach (column 5). It is observed that the method yields satisfactory results. In addition, Table 1 contains the corresponding errors in the simple beam theory solutions (column 4).

The important conclusions to be drawn from Figures 5 through 7 is that the problem of shear lag is insensitive to the ratio of flange moment of inertia to total moment of inertia; the type of loading has some minor effect and for earthquake type loadings Figure 7 would be the more appropriate curve to use; and finally, that the length of beam to width ratio determines the importance of shear lag in box beams.

ROTARY INERTIA AND SHEAR DEFORMATION EFFECTS ON BEAM MASS

For beams with large radius of gyration to length ratios, r/L, the error in the Bernoulli-Euler theory is considerable even for the lower modes. These discrepancies can be overcome by using the Timoshenko beam theory, whereby the effects of rotatory inertia and shear deformations are introduced. Also in developing lumped mass models it is common practice to assign masses only to translational degrees of freedom. Herein, an attempt is made to define a diagonal mass matrix, which would include shear and rotatory terms in it.

In the literature one may find consistent element mass matrices which contain the effects of shear deformations and rotatory inertia (4). Such a mass matrix is given in Appendix I, where $r^2 = I/A$, $\phi = 12EI/GA_s\ell^2$, ρ = mass density of the beam, A = cross-sectional area, A_s = shear area of the beam, ℓ = length of the beam segment, I = moment of inertia, E and G are respectively Young's and shear moduli of the beam material. To obtain an equivalent diagonal element mass matrix, a simple procedure is attempted: It is assumed that to each degree-of-freedom direction only the deflections which are compatible with that direction contribute (e.g., in U_1 direction U_1 and U_3 contribute); then their contributions are added to obtain a diagonal term (Eqn. Ib, Appendix I). This process results in $\rho A\ell/2$ for the term associated with the translational degrees of freedom. The same results are obtained by the usual concept of rigidly lumping of mass by tributary lengths. Since in the consistant mass matrix shear deformation effects impact on both the translational and rotatory inertia terms, it would be useful to consider rotatory inertia effects alone. Thus setting $G = \infty$ or $\phi = 0$, the "lumped" rotatory inertia term on the "diagonalized" element mass matrix becomes

$$J_{consistent} = \rho A\ell\left(\frac{\ell^2}{420} + \frac{r^2}{10}\right) \tag{19}$$

A comparison of Eqn. 19 with the one obtained by the rigid lumping concept would be useful. The corresponding term in the mass matrix for the latter approach for a segment of a rectangular section is given by

$$J_{rigid} = \frac{1}{2}\rho A\ell\left(\frac{\ell^2 + b^2}{12}\right) = \frac{1}{2}\rho A\ell\left(\frac{\ell^2}{12} + r^2\right) \tag{20}$$

Eqn. 20 would give significantly larger values than Eqn. 19. To illustrate the impact of this difference on the frequencies of a beam, the Timoshenko beam equation is modified to include rotatory inertia and bending effects only. The resulting frequencies are then compared with a lumped mass model using both Eqns. 19 and 20 to calculate rotatory inertia terms. The results for Beam 1 (refer to Table 2 for beam properties) are shown in Fig. 8. It is obvious that the concept of rigid lumping is more appropriate, suggesting a revision of the m_{22} and m_{44} terms of Eqn. Ib of Appendix I as follows

$$m_{22} = m_{44} = \frac{\left(\frac{\ell^2}{24} + \frac{r^2}{2}\right) + \frac{\phi^2 r^2}{2}}{(1+\phi)^2} \tag{21}$$

EAM MASS

ength ratios, r/L, the
le even for the lower modes.
Timoshenko beam theory,
deformations are introduced.
practice to assign masses only
ttempt is made to define
and rotatory terms in it.

ment mass matrices which
tory inertia (4). Such
/A, $\phi = 12EI/GA_s\ell^2$,
area, A_s = shear area of
nt of inertia, E and G are
material. To obtain an
procedure is attempted:
tion only the deflections
e (e.g., in U_1 direction
e added to obtain a
results in $\rho A\ell/2$ for
of freedom. The same
y lumping of mass by
trix shear deformation
ry inertia terms, it
s alone. Thus setting
on the "diagonalized"

(19)

by the rigid lumping
the mass matrix for the
ion is given by

$$\frac{\ell^2}{12} + r^2\Big) \qquad (20)$$

than Eqn. 19. To illus-
ies of a beam, the
atory inertia and bending
mpared with a lumped
otatory inertia terms.
operties) are shown in
ping is more appropriate,
n. Ib of Appendix I as

(21)

and resulting in the mass matrix of Eqn. Ic, Appendix I. For other than rectangular sections, the terms in parenthesis in the numerator should be interpreted as the polar mass moment of inertia about the nodal points.

To check the adequacy of the derived lumped mass matrix (Eqn. Ic, Appendix I), two uniform beams of constant properties throughout are selected with large r/L ratios to emphasize both the shear and rotatory effects. The properties of these beams are listed in Table 2. The beams are modeled as lumped mass models with equidistant nodes and the resulting frequencies for several number of lumped masses are compared to the theoretical results using the Timoshenko beam solution. The results are shown graphically in Figures 9 and 10. Both figures indicate that the lumped mass model frequencies will be within 10% of the theoretical frequencies if the number of masses are equal to N + 1, where N is the number of the desired Nth frequency.

It is instructive to compare Eqns. 20 and 21. Since ϕ is usually a large number for the type of structures considered, the effect of shear deformations on the mass matrix is small, which is as it should be. A study of the Timoshenko beam equation reveals that the translational and rotatory masses are dominant in the inertia effects and that shear deformations are dominant in the stiffness effects.

EVALUATION OF THE MODELING CONCEPT

To evaluate the adequacy of the modeling concepts developed in the paper, the response of a lumped mass model will be compared to that of a finite element model of the same structure. A symmetric box-type two story structure without openings is chosen with dimensions and properties such that the considerations discussed in this paper are accentuated. The structure with both finite element and lumped mass models is shown in Fig. 11. A modulus of elasticity of 51,800 Kips/ft^2 (2.5 x 10^6 N/m^2), a unit weight of 0.145 Kips/ft^3 (197 N/m^3) and Poisson's ratio of 0.17 is used. To make the comparison between the two models compatible, centerline dimensions are used in calculating the properties of the lumped mass model since the finite element model allows only such an analysis. The shell element used in the finite element model is a thin plate element having both membrane and bending isotropic properties (Kirchhoff hypothesis).

The lumped mass model was developed as follows:

a. The shear center and the centroid of the section coincide since the structure has double symmetry.

b. Effective shear area: The area associated with the finite-element model dimensions is given by A = 2 (20 x 1 + 40 x 1) = 120 ft^2 (11.2m^2). Using the Cowper (1) equation K = 0.234 and therefore A_s = 0.234 x 120 = 28.1 ft^2 (2.6 m^2). As shown in Fig. 2 and discussed earlier in the paper the Cowper equation needs to be re-evaluated for certain values of M and N. Thus the shear area is limited to 0.844 (2x20) = 33.8 ft^2 (3.1 m^2). However, using the Ebner and Billington equation (2), A_s = 37.3 ft^2 (3.5 m^2). Two models will be developed using shear areas of 33.8 ft^2 (3.1 m^2) and 37.3 ft^2 (3.5 m^2) respectively.

c. Shear lag effects: Using Fig. 7, for L/w = 1.5, I_f = 8000 ft^4 (69.2 m^4) and I = 9333 ft^4 (80.7 m^4), the flange stiffness reduction factor is given as β = 0.53. Thus the effective moment of inertia of the section is equal to 0.53 x 8000 + 1333 = 5573 ft^4 (48.2 m^2).

d. Mass matrix: From Eqn. Ic (Appendix I) the translational masses are simply obtained by lumping half of each element mass to the adjoining nodes. The floor masses will be assumed concentrated at the floor nodes. Thus the mass matrix elements associated with coordinates 1 through 6 are given by 2.7, 2.7, 6.3, 2.7, 2.7, and 4.95. The terms for rotatory inertia and shear effects can be simplified when it is recognized that for this example ϕ is a large number compared to unity. Thus a very good approximation to these terms can be obtained by $r^2/2$. This simplication serves to eliminate indirectly an issue raised in the calculation of shear areas. A second issue that should be resolved is the question of the shear lag effects on the calculation of the rotatory inertia terms. Among many possibilities two will be employed: a) the full cross-section properties and b) the partial cross-section properties. For the former the square of the radius of gyration is equal to r^2 = 9333/120 = 77.8 ft^2 (7.24 m^2) and for the latter r^2 = 5573/82.4 = 67.6 ft^2 (6.29 m^2). The cross-sectional area used in the latter is related to the reduced flange moment of inertia in an average sense. Thus, the effective area is obtained as 2 x 20 + 2 x 0.53 x 40 = 82.4 ft^2 (7.66 m^2). Similarly the mass per unit length (ρA) should reflect the same considerations. Thus for the first case $\rho A\ell$ = 0.145 x 120 x 5 + 32.2 = 2.7 and for the second case $\rho A\ell$ = 0.145 x 82.4 x 5 + 32.2 = 1.86. A similar consideration should be given the slabs. Although the slabs can be assumed to be rigid for translatory motion, they may not be so assumed for rotatory motion. Using Eqn. 20, for the first case $J = 3.6\,(1^2 + 20^2)/12 = 120$. Considering the effects of shear lag, it is reasonable to assume that the portion of the slab that, on the average, is affected by shear lag be excluded. This is simply effected by 0.53 x 120 = 63.6. From the above results the mass matrix elements associated with coordinates 7 through 12 for the first case are calculated as 210, 210, 330, 210, 210, and 225, and for the second case as 126, 126, 189, 126, 126, and 127.

The differences between the shear areas as given by Cowper and Ebner and Billington and between the two concepts of calculating the mass matrix result in four possible lumped mass models. The frequencies of these models are compared in Table 3. It is seen that the effect of using either shear area is negligible. And, except for the third mode, the effect of considering shear lag effects on the rotatory inertia terms is also negligible. (The participation factor of this third mode is extremely small.) Thus the model using the Cowper shear coefficients and neglecting the possible effects of shear lag on rotatory inertia terms would be considered as representative and compared to the finite element model. Since the finite-element model would result in many frequencies that, by the very nature of discrete modeling, are absent from the lumped mass models, an appropriate comparison between the finite-element model and the lumped mass models would be the response spectra of some representative point on the structure. The mid-point of the roof slab is selected for the purposes of this comparison.

These results are shown in Fi
selected to emphasize the dif
observed that the differences
model results are minor and a
remembered that the degree of
two orders of magnitude. The
1000 dynamic degrees of freed
lumped mass model.

CONCLUSIONS

From the several results
simple dynamic models can be
of box-type structures. The
include effects of shear lag
effects graphical solutions a
parameters affecting shear la
The question of shear area ne
formulations give adequate re
in the mass matrix and the as
gives acceptable results. Sh
minor and could be neglected.
effect of shear lag on the in
problem be evaluated on a cas

ACKNOWLEDGEMENTS

The authors thank their
and critical review of the pa
shear center for closed secti
problem and R. S. Platoni for

1. Cowper, G.R. "The Shear C
J. App. Mech., June 1966,
2. Ebner, A.M. and Billingto
Timoshenko's Beams." Jou
Vol. 94, No. ST3, March 1
3. Mindlin and Deresiewing "
Tech. Report No. 10, ONR
4. Przemieniechi, J.S., Theo
Book Co., New York, 1968.
5. Reissner, E. "Analysis of
Minimum Potential Energy,
6. Seely, F.B. and Smith, J.
Section Edition, John Wil
7. Tabakman, H.D., "Locating
Product Engineering, June
8. Timoshenko, S.P. Strength
D. Van Hostrand Co., New

= 1.5, I_f = 8000 ft^4 (69.2 m^4)
ess reduction factor is given
ertia of the section is equal

ie translational masses are
it mass to the adjoining nodes.
at the floor nodes. Thus the
es 1 through 6 are given by
for rotatory inert a and shear
d that for this example ϕ is
good approximation to these
ion serves to eliminate
of shear areas. A second issue
shear lag effects on the
ong many possibilities two will
rties and b) the partial cross-
of the radius of gyration
and for the latter
s-sectional area used in the
of inertia in an average sense.
+ 2 x 0.53 x 40 = 82.4 ft^2
(ρA) should reflect the same
0.145 x 120 x 5 + 32.2 = 2.7
+ 32.2 = 1.86. A similar
ough the slabs can be assumed
ot be so assumed for rotatory
= 3.6 $(1^2 + 20^2)/12$ = 120.
asonable to assume that the
ffected by shear lag be
20 = 63.6. From the above
th coordinates 7 through 12
330, 210, 210, and 225, and
, and 127.

s given by Cowper and Ebner and
culating the mass matrix
he frequencies of these models
effect of using either shear
mode, the effect of consider-
terms is also negligible.
s extremely small.) Thus the
neglecting the possible effects
e considered as representative
e the finite-element model
very nature of discrete
ls, an appropriate comparison
i mass models would be the
on the structure. The mid-point
of this comparison.

These results are shown in Fig. 12. The 1% damping response spectra was selected to emphasize the differences between the two basic models. It is observed that the differences between the finite-element and lumped mass model results are minor and acceptable in an engineering sense. It must be remembered that the degree of refinement in the two models differ by about two orders of magnitude. The finite element model has about 200 nodes and 1000 dynamic degrees of freedom as against 12 degrees of freedom for the lumped mass model.

CONCLUSIONS

From the several results shown in the paper it is concluded that simple dynamic models can be used in the prediction to seismic excitations of box-type structures. The stiffness properties of such structures should include effects of shear lag and the proper shear areas. For the shear lag effects graphical solutions are provided and it is observed that the important parameters affecting shear lag is the height to width ratio of the structure. The question of shear area needs further exploration although existing formulations give adequate results. Rotatory inertia terms should be included in the mass matrix and the assumption that the segment considered is rigid gives acceptable results. Shear deformation effects on the mass matrix are minor and could be neglected. In the absence of conclusive results of the effect of shear lag on the inertial masses it is recommended that the problem be evaluated on a case by case basis.

ACKNOWLEDGEMENTS

The authors thank their colleagues Y. J. Lin for his helpful suggestions and critical review of the paper, H. D. Tabakman for the computation of the shear center for closed sections, R. C. Lee for the results of the sample problem and R. S. Platoni for the results of Fig. 8.

REFERENCES

1. Cowper, G.R. "The Shear Coefficient in Timoshenko's Beam Theory" J. App. Mech., June 1966, pp. 335-340.
2. Ebner, A.M. and Billington, D.P. "Steady State Vibration of Damped Timoshenko's Beams." Journal of the Structural Division, ASCE, Vol. 94, No. ST3, March 1968, pp. 737-759.
3. Mindlin and Deresiewing "Timoshenko's Shear Vibrations of Beams" Tech. Report No. 10, ONR Project NR-064-388, Columbia Univ. 1953.
4. Przemieniechi, J.S., Theory of Matrix Structural Analysis, McGraw-Hill Book Co., New York, 1968.
5. Reissner, E. "Analysis of Shear Lag in Box Beams by the Principle of Minimum Potential Energy," Appl. Math., Vol. IV, No. 3, 1946, pp 268-278.
6. Seely, F.B. and Smith, J.O. Advanced Mechanics of Materials, Section Edition, John Wiley & Sons, New York, 1955, pp 97-111.
7. Tabakman, H.D., "Locating the Shear Center in Thin Closed Sections": Product Engineering, June 1954, pp. 137-141.
8. Timoshenko, S.P. Strength of Materials - Part I. Second Edition. D. Van Hostrand Co., New York, 1940, pp. 170-171.

Table 1. DISPLACEMENT ERROR ANALYSIS OF PRESENT APPROACH

LOADING TYPE (1)	FLANGE MOM. INERTIA / TOTAL MOM. INERTIA (2)	BEAM LENGTH / 1/2 FLANGE WIDTH (3)	MAX. % ERROR IN SIMPLE BEAM (4)	MAX. % ERROR IN MODIFIED SIMPLE BEAM (PRESENT APPROACH) (5)
POINT LOAD	0.85	5.0	13.0	6.53
	0.6	1.41	30.00	3.9
	0.667	1.41	34.47	4.75
	0.75	1.41	39.08	6.08
	0.85	0.92	56.64	5.41
UNIFORMLY DIST LOAD	0.5	5.0	10.80	4.18
	0.6	1.41	34.89	5.85
	0.667	1.41	39.08	7.07
	0.77	1.41	45.79	9.4
	0.86	0.92	59.97	8.20
TRIANGULAR DIST LOAD	0.5	5.0	9.58	4.18
	0.6	1.41	33.83	5.55
	0.667	1.0	44.00	4.7
	0.82	0.9	56.5	6.77

Table 2. BEAM PROPERTIES

	r/L	L (ft)	I (ft^4)	A (ft^2)	K	E (k/ft^2)	G (k/ft^2)	γ (k/ft^3)	ν
BEAM I	0.6	100	8,305,259	2,336	0.5	4.32×10^5	1.85×10^5	0.15	0.17
BEAM II	1.0	100	5.0×10^7	5.0×10^3	0.833	4.32×10^5	1.85×10^5	0.15	0.17

Table 3. FREQUENCY COMPARISON OF FOUR LUMPED MASS MODELS

MODES	NO SHEAR LAG EFFECTS ON MASS MATRIX		WITH SHEAR LAG EFFECTS ON MASS MATRIX	
	$A_S = 37.3$	$A_S = 33.8$	$A_S = 37.3$	$A_S = 33.8$
1	6.17	5.99	6.22	6.03
2	17.15	16.64	18.06	17.45
3	30.37	29.34	37.16	36.04
4	40.03	38.34	40.51	38.72
5	49.40	47.16	49.95	47.64
6	59.43	58.83	68.15	64.95

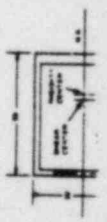

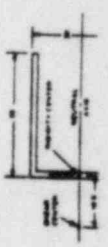

IS OF PRESENT APPROACH

TH / E	MAX. % ERROR IN SIMPLE BEAM (4)	MAX. % ERROR IN MODIFIED SIMPLE BEAM (PRESENT APPROACH) (5)
	13.0	6.53
	30.00	3.8
	34.47	4.75
	39.08	6.08
	55.64	5.47
	10.80	4.18
	34.89	5.85
	39.08	7.07
	45.79	9.4
	59.97	8.30
	9.58	4.18
	33.83	5.55
	44.00	4.7
	56.5	6.77

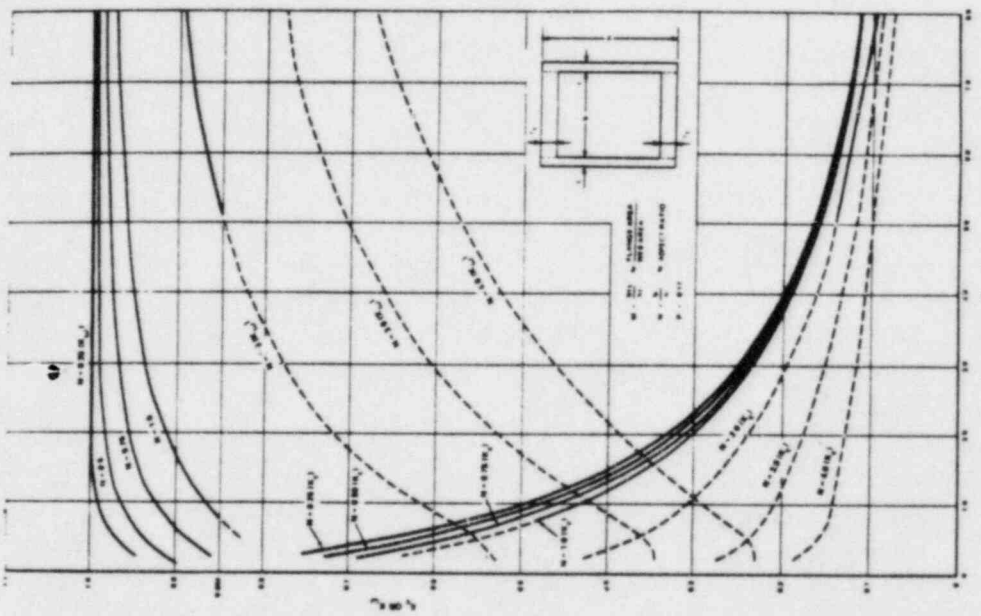

Table 2. SHEAR AREA COEFFICIENTS FOR BOX SECTIONS (AFTER COWPER (1))

ERTIES

K	E (k/ft^2)	G (k/ft^2)	γ (k/ft^3)	ν
.5	4.32×10^5	1.85×10^5	0.15	0.17
333	4.32×10^5	1.85×10^5	0.15	0.17

OUR LUMPED MASS MODELS

WITH SHEAR LAG EFFECTS ON MASS MATRIX	
A_S = 37.3	A_S = 33.8
6.22	6.03
18.06	17.45
37.16	36.04
40.51	38.72
49.95	47.64
68.15	64.95

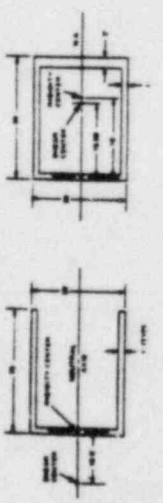

Figure 1. RIGIDITY AND SHEAR CENTER COMPARISON

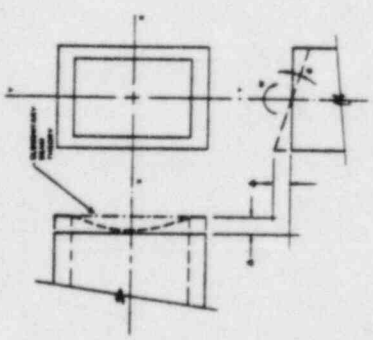

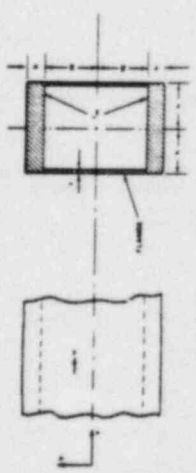

Figure 3. SHEAR LAG EFFECTS SCHEMATICALLY SHOWN

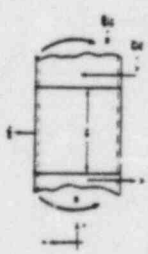

Figure 4. SKETCH OF ELEMENT OF BOX BEAM (USING REISSNER NOTATION)

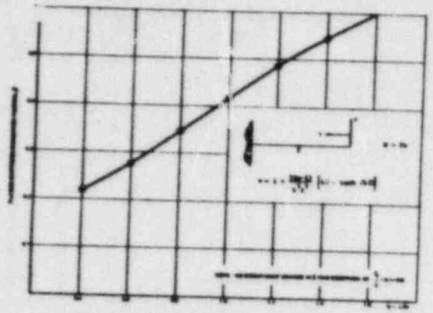

Figure 5. β VERSUS η, CANTILEVER – POINT LOAD

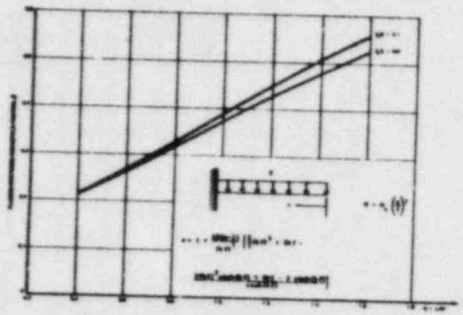

Figure 6. β VERSUS η, CANTILEVER – UNIFORMLY DISTRIBUTED LOAD

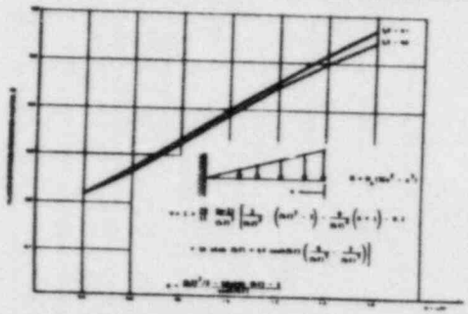

Figure 7. β VERSUS η, CANTILEVER – TRIANGULAR LOAD

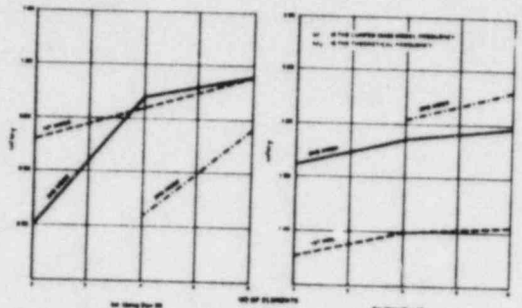

Figure 8. BEAM I CONVERGENCE STUDY – ROTATORY EFFECTS ONLY

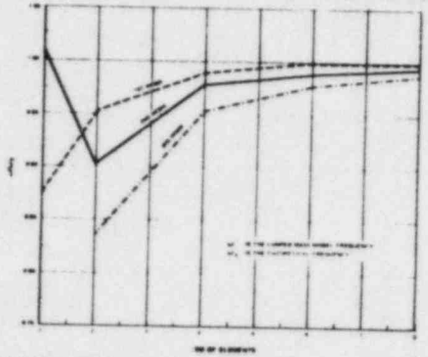

Figure 9. BEAM I CONVERGENCE STUDY – SHEAR AND ROTATORY EFFECTS

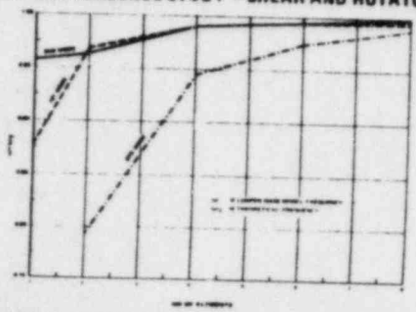

Figure 10. BEAM II CONVERGENCE STUDY – SHEAR AND ROTATORY EFFECTS

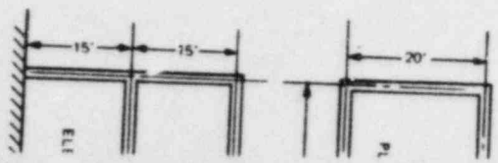

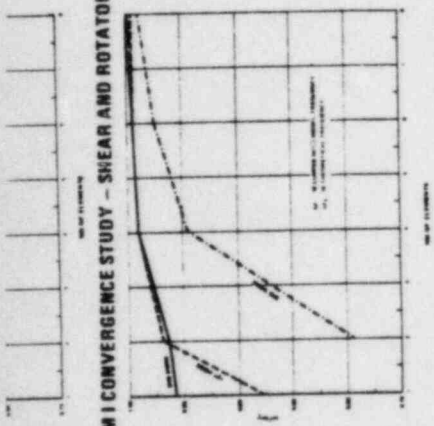

Figure 9. BEAM I CONVERGENCE STUDY – SHEAR AND ROTATORY EFFECTS

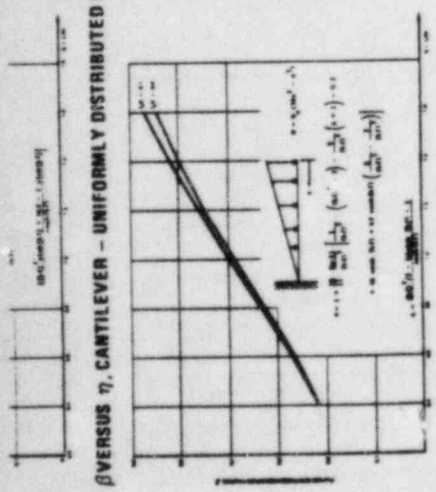

Figure 8. β VERSUS η, CANTILEVER – UNIFORMLY DISTRIBUTED LOAD

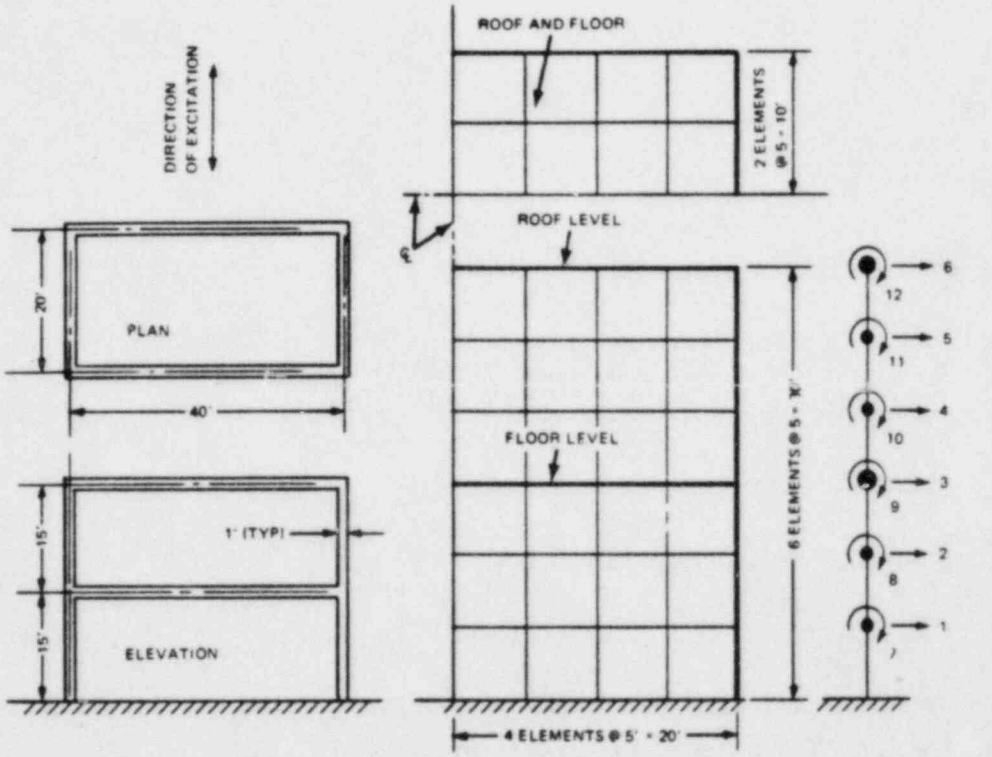

Figure 10. BEAM II CONVERGENCE STUDY – SHEAR AND ROTATORY EFFECTS

Figure 11 SCHEMATIC REPRESENTATION OF SAMPLE PROBLEM

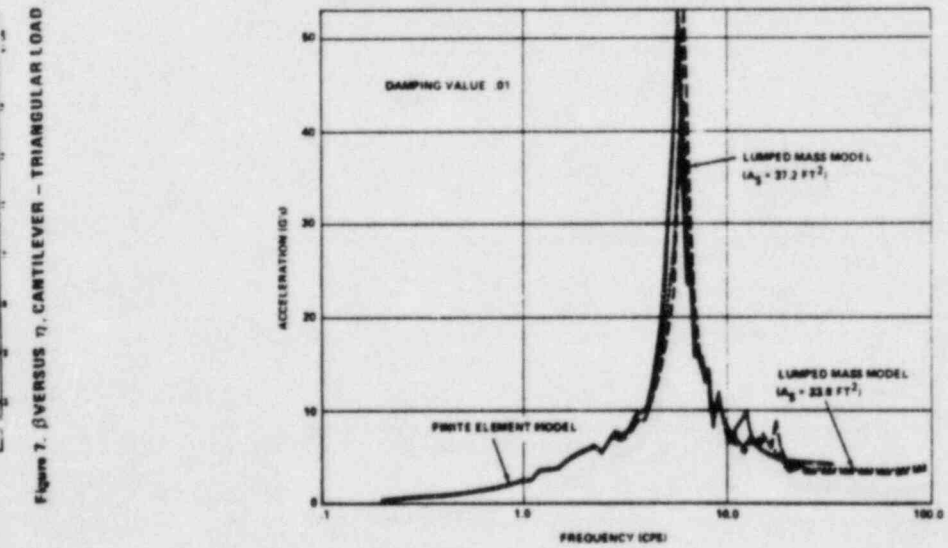

Figure 7. β VERSUS η, CANTILEVER – TRIANGULAR LOAD

Figure 12 RESPONSE SPECTRA COMPARISON OF FINITE ELEMENT AND LUMPED MASS MODEL, CENTER OF ROOF

APPENDIX I

Ia. CONSISTANT ELEMENT MASS MATRIX (4)

$$m = \frac{\rho A \ell}{(1+\Phi_s)^2}\begin{bmatrix} \frac{13}{35}+\frac{7}{10}\Phi_s+\frac{1}{3}\Phi_s^2 & & \text{Symmetric} & \\ \left(\frac{11}{210}+\frac{11}{120}\Phi_s+\frac{1}{24}\Phi_s^2\right)\ell & \left(\frac{1}{105}+\frac{1}{60}\Phi_s+\frac{1}{120}\Phi_s^2\right)\ell^2 & & \\ \frac{9}{70}+\frac{3}{10}\Phi_s+\frac{1}{6}\Phi_s^2 & \left(\frac{13}{420}+\frac{3}{40}\Phi_s+\frac{1}{24}\Phi_s^2\right)\ell & \frac{13}{35}+\frac{7}{10}\Phi_s+\frac{1}{3}\Phi_s^2 & \\ -\left(\frac{13}{420}+\frac{3}{40}\Phi_s+\frac{1}{24}\Phi_s^2\right)\ell & -\left(\frac{1}{105}+\frac{1}{60}\Phi_s+\frac{1}{120}\Phi_s^2\right)\ell^2 & -\left(\frac{11}{210}+\frac{11}{120}\Phi_s+\frac{1}{24}\Phi_s^2\right)\ell & \left(\frac{1}{140}+\frac{1}{60}\Phi_s+\frac{1}{120}\Phi_s^2\right)\ell^2 \end{bmatrix}$$

$$+\frac{\rho A \ell}{(1+\Phi_s)^2}\left(\frac{r}{\ell}\right)^2\begin{bmatrix} \frac{6}{5} & & \text{Symmetric} & \\ \left(\frac{1}{10}-\frac{1}{2}\Phi_s\right)\ell & \left(\frac{2}{15}+\frac{1}{6}\Phi_s+\frac{1}{3}\Phi_s^2\right)\ell^2 & & \\ -\frac{6}{5} & \left(-\frac{1}{10}+\frac{1}{2}\Phi_s\right)\ell & \frac{6}{5} & \\ \left(\frac{1}{10}-\frac{1}{2}\Phi_s\right)\ell & \left(-\frac{1}{30}-\frac{1}{6}\Phi_s+\frac{1}{6}\Phi_s^2\right)\ell^2 & \left(-\frac{1}{10}+\frac{1}{2}\Phi_s\right)\ell & \left(\frac{2}{15}+\frac{1}{6}\Phi_s+\frac{1}{3}\Phi_s^2\right)\ell^2 \end{bmatrix}$$

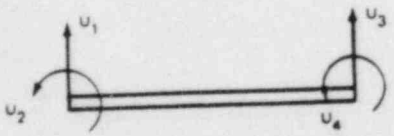

$$\Phi_s = 12EI/GA_s\ell^2$$

Ib. "LUMPED" ELEMENT MASS MATRIX FROM Ia ABOVE.

$$m = \rho A \ell \begin{bmatrix} \frac{1}{2} & & \frac{1}{2} & \\ \frac{\frac{\rho^2}{420}+\frac{r^2}{10}+\frac{\rho^2 r^2}{2}}{(1+\Phi)^2} & & \frac{\frac{\rho^2}{420}+\frac{r^2}{10}+\frac{\rho^2 r^2}{2}}{(1+\Phi)^2} & \end{bmatrix}$$

Ic. MODIFIED "LUMPED" ELEMENT MASS MATRIX

$$m = \rho A \ell \begin{bmatrix} \frac{1}{2} & & \frac{1}{2} & \\ \frac{\left(\frac{\rho^2}{24}+\frac{r^2}{2}\right)+\frac{\rho^2 r^2}{2}}{(1+\Phi)^2} & & \frac{\left(\frac{\rho^2}{24}+\frac{r^2}{2}\right)+\frac{\rho^2 r^2}{2}}{(1+\Phi)^2} & \end{bmatrix}$$

INELAST

GEORGE N
Senior Struc

This pape
the effect of imp
structural walls
of vibration as a
in the post yield

The basic
corresponding a
at floor levels.
the ends of elem
characteristics
from cyclic load
component of th
to obtain a 5% d
of the El Centro

The effec
is evaluated es
requirements o
height of the bu
and thus decre
displacements t
the yield level
the magnitude

In recen
have indicated
the structures

Rotational Mass $$m_r = \left[\frac{l^2}{24} + \frac{r^2}{2} + \frac{\phi^2 r^2}{2}\right] \frac{A\rho l}{(1+\phi)^2}$$

$$\phi = \frac{24(1+\nu)I}{A_s l^2}$$

Paper states:

$$m = \left[\frac{\left(\frac{l^2}{24} + \frac{r^2}{2}\right) + \frac{\phi^2 r^2}{2}}{(1+\phi)^2}\right] \rho A l \qquad \text{(eq. 21, app. I)}$$

AND $$\phi = \frac{12EI}{GA_s l^2}$$

HOWEVER,

$$G = \frac{E}{2(1+\nu)}$$

∴ SUBSTITUTING THIS EXPRESSION IN $\phi = \frac{12EI}{GA_s l^2}$ YIELDS:

$$\phi = \frac{12EI}{\left[\frac{E}{2(1+\nu)}\right] A_s l^2} = \frac{24(1+\nu)I}{A_s l^2}$$

Enclosure 7

ADDITIONAL INFORMATION REQUIRED FOR SATISFACTORY

QUESTION RESPONSE

Q220.5	Revise response concerning properly prepared construction joints ensuring leaktightness to include supporting reference data.
Q220.8	Revise response (Table 220.8-1) so that for flexure, slabs with two-way reinforcing, the Vogtle design criteria is identical to ACI 349, Appendix C, as modified by RG 1.142.
Q220.9	Provide justification for the formula in Table 220.9-1, Footnote a.
Q220.15	Revise response to indicate that the fixed-base natural frequencies for major Category 1 structures are provided in the design reports.
Q220.21	Revise response to indicate that the seismic instrumention inservice surveillance program is in agreement with the provisions in the standard Technical Specifications.
Q220.22	Revise response to include reference to the appropriate FSAR section.
Q220.26/ Q220.27	Revise response to address the 12 positions listed in RG 1.142.

SECOND SYMPOSIUM
ON
EARTHQUAKE ENGINEERING

Sponsored by the

UNIVERSITY GRANTS COMMISSION

SCHOOL OF RESEARCH AND TRAINING
IN
EARTHQUAKE ENGINEERING
UNIVERSITY OF ROORKEE
ROORKEE (U.P.) INDIA

(November 10–12, 1962)

EARTHQUAKE RESISTANT DESIGN OF RETAINING WALLS

I. P. Kapila *

SYNOPSIS

This paper relates the determination of active and passive pressures exerted by cohesionless meterial under earthquake conditions. The introduction of earthquake inertia forces to Coulomb's sliding wedge yields the Mononobe-Okabe formula. Modifications of known graphical methods to include the effect of earthquake forces are presented in this paper.

INTRODUCTION

The pressure, both active and passive, exerted by cohesionless material against a retaining structure in the absence of earthquake conditions may be determined by the well known Coulomb's Wedge Theory. The earthquake problem introduces an inertia force corresponding to the acceleration imparted to the mass of the sliding wedge. The solution of the resulting force diagram yields the pressure exerted against the the structure which can be expressed by the Mononobe-Okabe Formula (1, 2). Several graphical methods are available for pressure determination from Coulomb's Wedge Theory. Modification of two such methods are presented in this paper to include the effect of eathquake force.

ACTIVE PRESSURE

Coulomb's Formula : In Fig 1 (a). AB is the fill-side face of the retaining structure, inclined at an angle α to the vertical. The surface of the fill AD is inclined to the horizontal at an angle δ. If the retaining structure is removed, the material of the fill will settle finally at the angle of repose which is close to the angle of internal friction, represented by the plane BD. According to the Coulomb's Wedge Theory, however, when the retaining structure moves forward only slightly, the surface of rupture will not form at plane BD immediately. Instead, the plane of rupture will lie somewhere between AB and BD. It may be assumed to correspond to the plane BC in Fig. 1 (a). The active pressure against the retaining structure is caused by the weight of the wedge ABC (assuming earthquake force to be absent) and it is desired to determine the location of the plane BC which will cause the maximum reaction against the face AB.

(2)

* Director, Bhakra Beas Dam Design Directorate, New Delhi.

The reaction against the face AB will be inclined at an angle $\varnothing_1$ to the normal, where $\varnothing_1$ is the angle of wall friction between the cohesionless material and the face of the retaining structure. The reaction against the plane BC will be inclined at an angle $\varnothing$ to the normal.

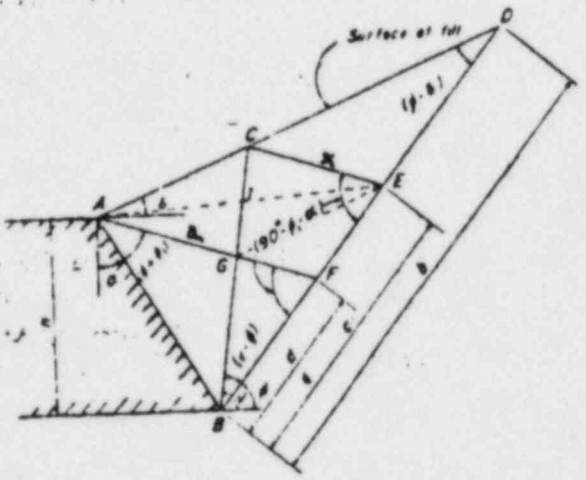

Fig. 1 (a)

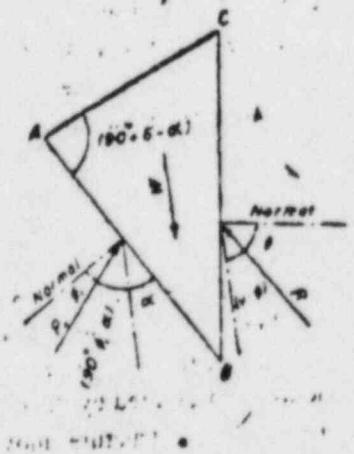

Fig. 1 (b)

Fig. 1 (c)

If these two reactions are designated P_A and R respectively and the weight of wedge is W, P_A may be determined from the triangle of forces Fig. 1 (c). If AF and CE in Fig. 1 (a) are drawn such that each makes an angle $(90° - \varnothing_1 - \alpha)$ with BD, it has been shown (3, 4) that the maximum active pressure would result when

$$\triangle ABC = \triangle BCE \qquad (1)$$

and

$$x = \frac{a\sqrt{b}}{\sqrt{b} + \sqrt{d}} \qquad (2)$$

(3)

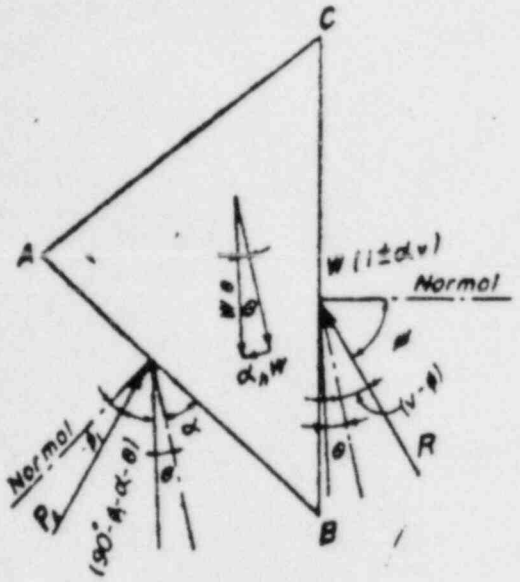

Fig. 2 (b)

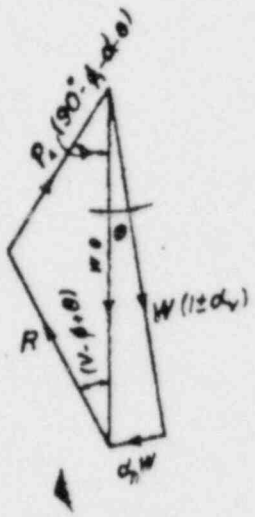

Fig. 2 (c)

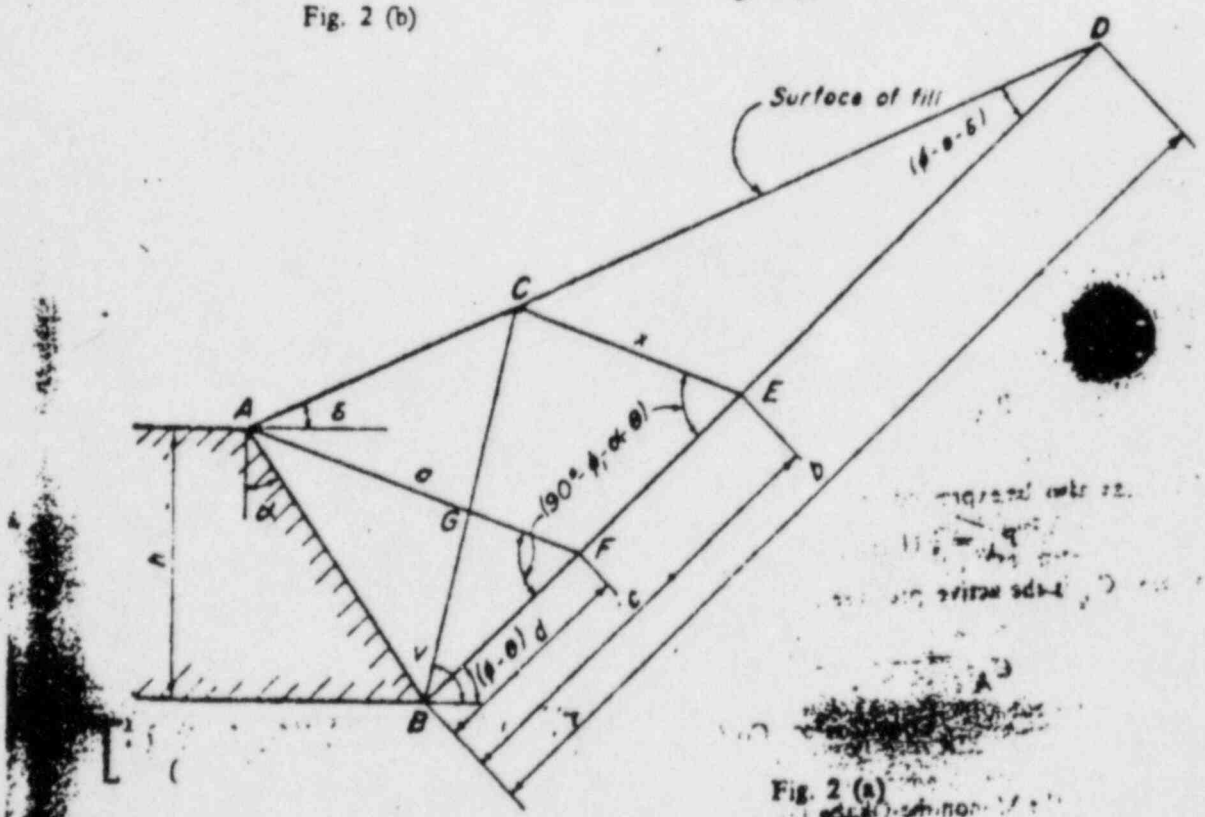

Fig. 2 (a)

the mazimum active pressure would be

$$= \tfrac{1}{2}\gamma x^2 \operatorname{Sin}[90 - (\alpha(^1\varnothing \quad +) \tag{3}$$

where γ is the unit weight of the cohesionless material. This may also be expressed as

$$P_A = \frac{\frac{1}{2}\gamma.h^2 \ \operatorname{Cos}^2(\varnothing - \alpha)}{\operatorname{Cos}^2\alpha. \ \operatorname{Cos}(\varnothing_1 + \alpha)\left[1 + \left\{\frac{\operatorname{Sin}(\varnothing + \varnothing_1)\operatorname{Sin}(\varnothing - \delta)}{\operatorname{Cos}(\varnothing_1 + \alpha)\operatorname{Cos}(\delta - \alpha)}\right\}^{\frac{1}{2}}\right]^2} \tag{4}$$

which is the Coulomb's Formula for active pressure.

The Mononobe-Okabe Formula : For earthquake conditions, additional inertia forces $\alpha_h W$ and $\pm \alpha_v W$ would be imposed on the mass of the sliding wedge (Fig. 2) where α_h and α_v are the horizontal and vertical seismic coefficients respectively. The resultant force, W_r, is thus

$$W_r = \frac{(1 \pm \alpha_v)\, W}{\operatorname{Cos}\theta} \tag{5}$$

where $$\theta = \tan^{-1}\frac{\alpha_h}{1 \pm \alpha_v} \tag{6}$$

According to the Mononobe's theory, the effect of the accelerations due to an earthquake is to modify the direction of the gravity force, which would be equivalent to a rotation of the vertical and horizontal planes of reference through an angle θ in the same direction. This effect may be introduced by plane BD making an angle $(\varnothing - \theta)$ with the horizontal as indicated in Fig. 2(a). The resulting force polygon would be as shown in Fig. 2 (c)

If AF and CE in Fig. 2 (a) are drawn such that each makes an angle $(90 - \varnothing_1 - \alpha - \theta)$ with BD, it can be shown that the maximum active pressure would result when the requirements of Eq. (1) and Eq. (2) as for the non-seismic condition are satisfied. The maximum active pressure would be

$$P_A = \tfrac{1}{2}\frac{(1 \pm \alpha_v).\gamma}{\operatorname{Cos}\theta} x^2. \operatorname{Sin}[90 - (\alpha + \varnothing_1 + \theta)] \tag{7}$$

This may also be expressed as

$$P_A = \tfrac{1}{2}(1 \pm \alpha_v)\gamma h^2 \ C_A \tag{8}$$

where C_A is the active pressure coefficient

$$C_A = \frac{\operatorname{Cos}^2(\varnothing - \alpha - \theta)}{\operatorname{Cos}\theta \operatorname{Cos}^2\alpha. \operatorname{Cos}(\varnothing_1 + \alpha + \theta)\left[1 + \left\{\frac{\operatorname{Sin}(\varnothing + \varnothing_1)\operatorname{Sin}(\varnothing - \delta - \theta)}{\operatorname{Cos}(\varnothing_1 + \alpha + \theta)\operatorname{Cos}(\delta - \alpha)}\right\}^{\frac{1}{2}}\right]^2}$$

This is the Mononobe-Okabe Formula for active pressure.

(5)

GRAPHICAL METHOD

Culmann's Method

Culmann's graphical method for the determination of active pressure is of more general application than sevral others described in text-books on Soil Mechanics. It essentially comprises the construction of the triangle of forces for each of the several assumed planes of rupture. The vector representing the weight of the wedge is plotted on plane I D, Fig. (1). The vector representing the active pressure is then drawn so as to make an angle $(90-\phi_1-\alpha)$ with the plane BD. The triangle of forces is thus that which is formed by the assumed plane of rupture, the plane BD and the active pressure vector drawn as indicated above. The locus of the point of intersection of the active pressure vector with the corresponding plane of rupture is designated as the "Culmann Line". The maximum distance between plane BD and the tangent to the Culmann Line drawn parallel to the plane BD, measured parallel to the active pressure vector is the active pressure to the force scale adopted in the construction.

The modifications necessary in Culmann's graphical construction to include the effect of earthquake forces would be readily apparent from the preceding discussion regarding the Mononobe—Okabe Formula. These are:—

i) The plane BD is to be drawn such that it is inclined at an angle $(\phi-\theta)$ to the horizontal.

ii) The active pressure vector is to be drawn at an angle $(90-\phi_1-\alpha-\theta)$ with the plane BD.

It would be seen that the resulting triangle of forces conforms to that shown in Fig. 2(c) This modification is illustrated in the example on Fig. 3.

Melbye's Method

Another graphical method based on Coulomb's Wedge Theory has been proposed by A. Melbye (4). This is directed towards drawing the plane of rupture such that the requirments of Eq. (1) are met, and then scaling off the length 'x' to the linear scale of the construction. In Fig. 1, if EG is drawn parallel to AD, then N must lie on the plane of rupture for Eq. 1 to be satisfied. Furthermore, it can be shown that the locus of the point 'I' (which is the intersection of the diagonals GC and AE of the parallelogram ACEG) will be parallel to BD and will bisect AB. The graphical construction, therefore, merely requires drawing a line which bisects AB and is parallel to BD, and then determinining by trial the plane of rupture BC which yields GI=IC. The modifications necessary to include the effect of earthquake forces would be,

(i) The plane BD is to be drawn so as to make an angle $(\phi-\theta)$ with the horizontal

(ii) AF is to be drawn to make an angle $(90-\phi_1-\alpha-\theta)$ with BD.

It would be seen that the requirements of Eq. (1) remain unchanged under the earthquake conditions. The value of 'x' as determined by this construction can be substituted into Eq. (7) to yeild maximum active pressure. The application of this method is illustrated in Fig. 4.

(6)

DATA :

$h = 100$ ft.
$\alpha = 35°$
$\phi = 30°$
$\phi_1 = 15°$
$\delta = 15°$
$\alpha_h = 0.15$ (acceleration away from retaining structure)
$\alpha_v = 0.05$ (acceleration downwards)
$\theta = 9°$
$\gamma = 132$ lbs,/cft.

Maximum active pressure vector = 930 kips

$$P_A = \frac{(1-0.05)}{\cos 9°} \cdot 930 \text{ kips}$$

$$= 894.5 \text{ kips}$$

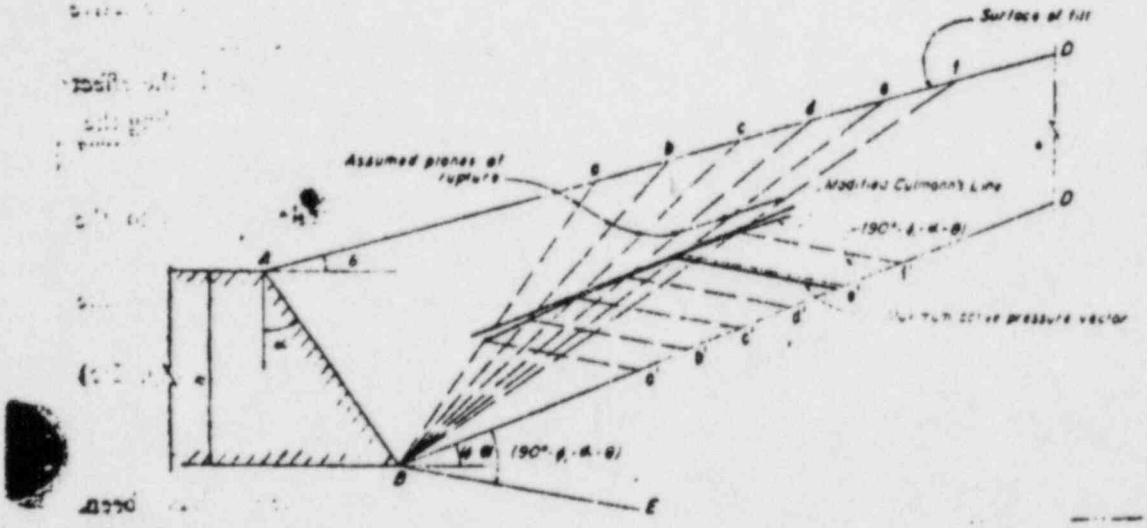

PROCEDURE

1. Draw BD to make an angle $(\phi - \theta)$ with the horizontal.
2. Assume planes of rupture Ba, Bb etc., and compute weight of wedge ABa, ABb etc. and plot on any convenient force scale Ba', Bb' on BD.
3. Draw active pressure vectors from a', b' etc. at an angle $(90° - \phi_1 - \alpha - \theta)$ with BD to intersect corresponding assumed planes of rupture.
4. Draw the locus of the intersection of assumed planes of rupture and corresponding active pressure vector (The Culmann Line) and determine the active pressure vector parallel to BE.

Fig. 3—Modified Culmann's Construction for Active Pressure.

DATA:

h = 100 ft.
α = 35°
$\varnothing$ = 30°
$\varnothing_1$ = 15°
δ = 15°
α_h = Acceleration away from retaining structu.e = 0.15
α_v = Acceleration downwards = 0.05
θ = 9°
γ = 132 lbs./cft.

$$P_A = \tfrac{1}{2}(1 \pm \alpha_v)\gamma x^3 \frac{\text{Cos.}(\varnothing_1 + \alpha + \theta)}{\text{Cos}\,\theta}$$

$$= \tfrac{1}{2}(1-0.05).\ 132.\ (165.5)^3 \frac{\text{Cos. } 59°}{\text{Cos. } 9°} \text{ lbs.}$$

$$= 895.6 \text{ kips}$$

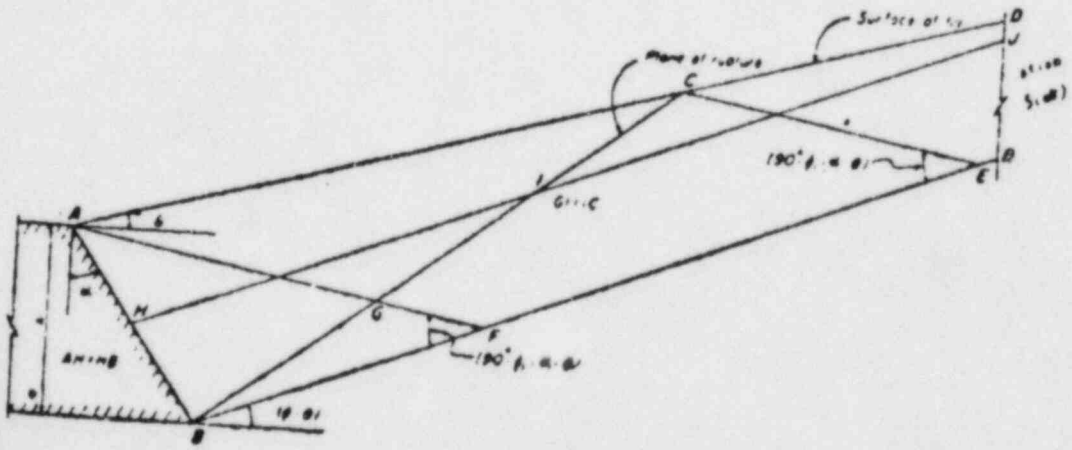

PROCEDURE

1. Draw BD to make an angle $(\varnothing - \theta)$ with the horizontal.
2. Bisect AB, AH = BH.
3. Draw HJ parallel to BD.
4. Draw AF to make an angle $(90° - \varnothing_1 - \alpha - \theta)$ with BD.
5. Determine plane of rupture BC by trial such that GI = IC.
6. Draw CE parallel to AF and measure length to linear scale of construction.

Fig. 4*—Modified Melbye's Construction for Active Pressure.

* Based on paper "Determining Active Thurst on the back of a Wall Retaining Cohesion-less Material" by A Melbye, Civil Engineering & Public Works Review Vol. 56, No. 660, July 1961.

PASSIVE PRESSURE

Coulomb's Formulae:—The determination of the passive pressure follows the same basic considerations as for active pressure, with the main point of difference being that the plane of rupture be such as will result in the minimum pressure against the retaining structure. The plane BD shown in Fig. 1 and 2 to be above the horizontal plane for the active pressure condition would be below the horizontal plane for passive pressure and horizontal earthquake inertia forces would have to be assumed acting away from the structure and not towards the structure.

$$P_p = \frac{1}{\cos\theta} \text{ (Minimum Passive Pressure Vector) } (1 \pm \alpha_v)$$

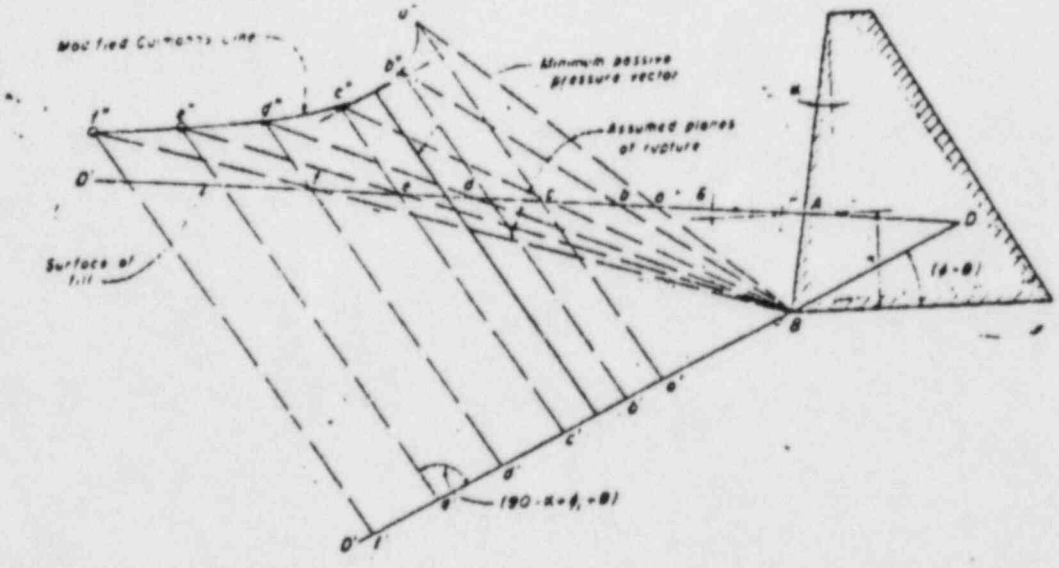

PROCEDURE

1 Draw DBD' to make angle $(\phi - \theta)$ with horizontal.

2 Assume planes of rupture Ba, Bb, etc. and compute weight of wedge ABa, ABb, etc. and plot Ba', Bb' to any convenient force scale on DBD'

3 Draw passive pressure vectors from a', b' etc. at an angle $(90 - \alpha + \phi_1 + \theta)$ to intersect corresponding assumed planes of rupture.

4 Draw the locus of the intersection of the assumed rupture planes and the corresponding passive pressure vectors (The Culmann Line) and determine the minimum passive pressure vector.

Fig. 5—Modified Culmann's Construction for Passive Pressure.

$$P_p = \tfrac{1}{2}\gamma . x^2 . \frac{\text{Cos.}\,(\varnothing_1 - \alpha + \theta)\,(1 \pm \alpha_v)}{\text{Cos}\,\theta}$$

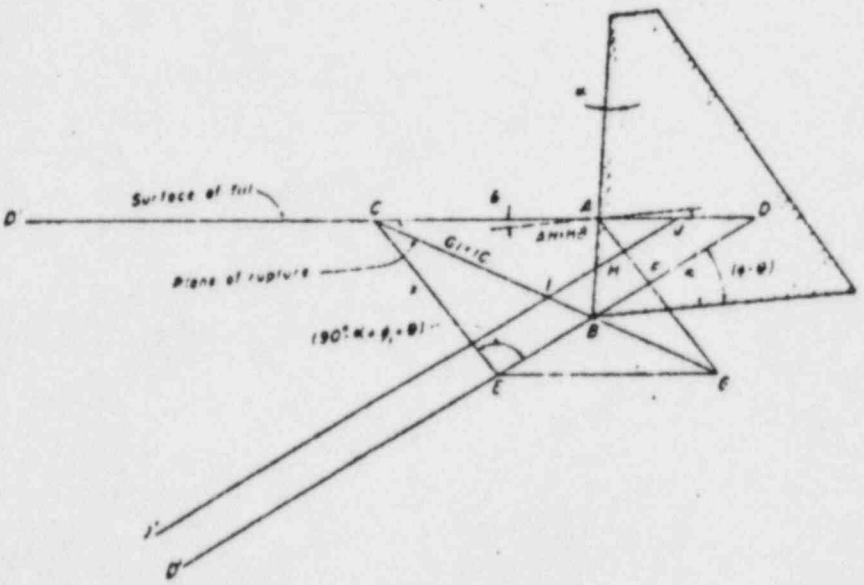

PROCEDURE

1. Draw DBD' to make an angle $(\varnothing - \theta)$ with the horizontal
2. Bisect AB, AH = BH.
3. Draw JHJ parallel to DBD'.
4. Draw A F G to make angle $(90° + \varnothing_1 - \alpha + \theta)$ with DBD'
5. Determine plane of rupture BC by trial such that GI = IC.
6. Draw CE parallel to AG and measure length to linear scale of construction.

Fig. 6—Modified Melbye's Construction for Passive Pressure.

The analytical solution for passive pressure due to cohesionless aterial would show that the requirements of Eq. (1) continue to hold and that whether earthquake forces are included in the analysis. For normal conditions, without uake, the passive pressure is

$$P_p = \tfrac{1}{2}\gamma\, x^2 \,\text{Cos}\,(\alpha - \varnothing_1) \qquad (10)$$

* Based on paper, "Determining Active Thrust on the back of a Wall Retaining Cohesion-less Material" by A. Melbye, Civil Engineering & Public Works Review Vol. 56, No. 660, July 1961.

(10)

This may also be expressed as

$$P_p = \frac{\frac{1}{2}\gamma.h^2 \cos^2(\alpha + \varphi)}{\cos^2\alpha \cos(\varphi_1 - \alpha)\left[1 - \left\{\frac{\sin(\varphi - \varphi_1)\sin(\varphi + \delta)}{\cos(\varphi_1 - \alpha)\cos(\alpha - \delta)}\right\}^{\frac{1}{2}}\right]^2} \quad (11)$$

The Mononobe–Okabe Formula

When earthquake inertia forces are included, the passive pressure is

$$P_p = \frac{1}{2}(1 \pm \alpha_v)\frac{\gamma.h^2}{\cos\theta}\cos.(\alpha - \varphi_1 - \theta) \quad \ldots \quad \ldots \quad \ldots \quad \ldots \quad (12)$$

Where θ is as defined in Eq. (6).

This may also be expressed as

$$P_p = \frac{1}{2}(1 \pm \alpha_v)\gamma.h^2.C_p \quad \ldots \quad \ldots \quad \ldots \quad \ldots \quad (13)$$

where C_p is the passive pressure coefficient

$$C_p = \frac{\cos^2(\varphi + \alpha - \theta)}{\cos\theta.\cos^2\alpha.\cos(\varphi_1 - \alpha + \theta)\left[1 - \left\{\frac{\sin(\varphi - \varphi_1)\sin(\varphi + \delta - \theta)}{\cos(\delta - \alpha)\cos(\varphi_1 - \alpha + \theta)}\right\}^{\frac{1}{2}}\right]^2} \quad (14)$$

This is the Mononobe-Okabe Formula for passive pressure.

GRAPHICAL METHODS

The Culmann and Melbye graphical methods for passive pressure determination follow the same basis described earlier, and the modifications considered necessary for active pressure would apply for including the effects of earthquake forces. The application of these two graphical methods for earthquake resistant design is indicated in Figs. 5 and 6.

REFEENCES;

1. Mononobe, N. and H. Matsuo, (1929), "On Determination of Earth Pressure During Earthquakes" Proceedings World Engineering Congress, Tokyo, 1929.

2. Okamoto, S., (1956) "Bearing Capacity of Sandy Soils and Lateral Earth Pressure during Earthquake", Proceedings of the World Conference on Earthquake Engineering, Berkeley, Calif. June 1956.

3. Kapila, J.P., and S.S. Maini, (1962), "Active Pressure Exerted by Cohesionless Materials under Earthquake Conditions." Indian Concrete Journal, Vol. 36, No. 5, May 1962.

4. Kapper, P.L. and W.F. Cassie, (1962), "The Mechanics of Engineering Soils" E and F.N. Spon, London.

5. Melbye, A., (1961) "Determining the Maximum Active Thrust on the Back of a Wall Retaining Cohesionless Material" Civil Engineering and Public Works Review Vol. 56. No. 660. July 1961.

MEETING SUMMARY DISTRIBUTION

Docket No(s): 50-424/425
NRC PDR
Local PDR
NSIC
PRC System
LB #4 r/f
Attorney, OELD
E. Adensam
Project Manager M. Miller
Licensing Assistant M. Duncan

NRC PARTICIPANTS

M. Miller
S. Chan
R. Lipinski

bcc: Applicant & Service List